NAVAL POSTGRADUATE SCHOOL
MONTEREY, CALIFORNIA

THESIS

DIRECTED ENERGY EFFECTS ON THE FLIGHT PATH OF A SPINNING BALLISTIC PROJECTILE

by

George S. Capen

June 1995

Thesis Co-Advisors: M. E. Melich
K.E. Woehler

Approved for public release; distribution is unlimited

REPORT DOCUMENTATION PAGE

Form Approved OMB No. 0704-0188

1. AGENCY USE ONLY *(Leave blank)*	2. REPORT DATE	3. REPORT TYPE AND DATES COVERED
	June 1995	Master's Thesis

4. TITLE AND SUBTITLE : DIRECTED ENERGY EFFECTS ON THE FLIGHT PATH OF A SPINNING BALLISTIC PROJECTILE

5. FUNDING NUMBERS

6. AUTHOR GEORGE S. CAPEN

7. PERFORMING ORGANIZATION NAME(S) AND ADDRESS(ES)
Naval Postgraduate School
Monterey CA 93943-5000

8. PERFORMING ORGANIZATION REPORT NUMBER

9. SPONSORING/MONITORING AGENCY NAME(S) AND ADDRESS(ES)

10. SPONSORING/MONITORING AGENCY REPORT NUMBER

11. SUPPLEMENTARY NOTES The views expressed in this thesis are those of the author and do not reflect the official policy or position of the Department of Defense or the U.S. Government.

12a. DISTRIBUTION/AVAILABILITY STATEMENT
Approved for public release;distribution is unlimited.

12b. DISTRIBUTION CODE

13. ABSTRACT *(maximum 200 words)*

This thesis will examine the equations of motion for a spinning ballistic projectile. The goal of such an examination is to determine the possible mechanisms by which a directed energy weapon may induce sufficient instability as to significantly alter the projectile's flight path. A ballistic projectile is generally launched with a "fire and forget" philosophy. The desired impact point is determined before firing. It may be possible to alter the projectile in such a way that it fails to follow the desired trajectory thereby missing the intended target. Several variables appear to be worthy of investigation to assess their contribution to a required instability or range reduction. Skin friction drag may be increased from surface roughness generated by a pulsed energy source. The results that this thesis will examine include: impulse generated by the laser interaction, additional Magnus effects and aerodynamic drag. Moment induced instability may also result from these in the form of a Magnus moment or drag torque. Increasing the drag force appears to be the most promising theoretical solution to defeating an incoming spinning ballistic projectile.

14. SUBJECT TERMS	15. NUMBER OF PAGES
Ballistic, Projectile, Laser, Directed Energy, Magnus, Drag, Yaw	96
	16. PRICE CODE

17. SECURITY CLASSIFICATION OF REPORT	18. SECURITY CLASSIFICATION OF THIS PAGE	19. SECURITY CLASSIFICATION OF ABSTRACT	20. LIMITATION OF ABSTRACT
Unclassified	Unclassified	Unclassified	UL

NSN 7540-01-280-5500

Standard Form 298 (Rev. 2-89)
Prescribed by ANSI Std. 239-18 298-102

Approved for public release; distribution is unlimited.

DIRECTED ENERGY EFFECTS ON THE FLIGHT PATH OF A SPINNING BALLISTIC PROJECTILE

George S. Capen
Lieutenant, United States Navy
B.S., United States Naval Academy, 1989

Submitted in partial fulfillment
of the requirements for the degree of

MASTER OF SCIENCE IN APPLIED PHYSICS

from the

NAVAL POSTGRADUATE SCHOOL
June 1995

Author: _____
George S. Capen

Approved by: _____
Michael E. Melich, Thesis Co-Advisor

_____
Karlheinz E. Woehler, Thesis Co-Advisor

_____
William B. Colson, Chairman
Department of Physics

ABSTRACT

This thesis will examine the equations of motion for a spinning ballistic projectile. The goal of such an examination is to determine the possible mechanisms by which a directed energy weapon may induce sufficient instability as to significantly alter the projectile's flight path. A ballistic projectile is generally launched with a "fire and forget" philosophy. The desired impact point is determined before firing. It may be possible to alter the projectile in such a way that it fails to follow the desired trajectory thereby missing the intended target. Several variables appear to be worthy of investigation to assess their contribution to a required instability or range reduction. Skin friction drag may be increased from surface roughness generated by a pulsed energy source. The results that this thesis will examine include: impulse generated by the laser interaction, additional Magnus effects and aerodynamic drag. Moment induced instability may also result from these in the form of a Magnus moment or drag torque. Increasing the drag force appears to be the most promising theoretical solution to defeating an incoming spinning ballistic projectile.

TABLE OF CONTENTS

TABLE OF VALUES

C_S	specific heat of steel	0.15 cal/gr-C
d	155mm projectile diameter	.155 m
g	acceleration due to gravity	9.8 m/sec^2
K_A	spin decelerating coefficient	.08
K_D	drag force coefficient	.004
K_H	damping moment coefficient	1.2
K_L	lift force coefficient	1.0
K_M	over turning moment coeff.	2.5
K_N	normal force coefficient	1.3
K_T	Magnus moment coefficient	0.3
L	155mm projectile length	70 cm
L_M	latent heat of melting	65 cal/gr
m	155mm projectile mass	45 kg
T_M	melting temperature of steel	1450 C
U	wind speed over the projectile	600 m/s
u_S	speed of sound in air	350 m/s
v	speed of the projectile	600 m/s
ω	155mm projectile spin frequency	220 hz
ρ_{air}	standard density of air	1.2 gr/cm^3
ρ_{steel}	density of steel	8 gr/cm^3

* Many of these terms are approximations based on diagrams and conversations with aerodynamics researchers at the Army Research Laboratory in Aberdeen, Maryland. The exactness of these values is not significant to the magnitude estimations in this thesis. Additional special case values will be introduced in the text.

I. INTRODUCTION

This thesis is directed toward solving a stated goal of the Defense Planning Guide. Our current armed forces are vulnerable to gunfire attack due to an antiquated counterbattery system of equipment and technique. Specifically, in today's battlefield, surgical precision is required and may involve protecting civilian lives in a confined suburban environment. There is a need to develop a new system using state of the art technology to destroy incoming projectiles minimizing loss of life. Laser technology has given us the ability to track, classify and engage incoming ballistic rounds to meet this goal. This thesis will explore the use of laser energy to accomplish the defeat of the projectile.

This mission responds to the Department of Defense "Defense Planning Guidance (DPG) for FY 1996-2001" dated 23 May 1994. This involves countering armor, mortar and mobile artillery threats to U.S. forces conducting an amphibious invasion, U.S. forces defending a coastal region from invasion and to coastal cities and safe zones under U.S. protection during peace keeping operations. There are several specific guidelines in the DPG:

- "U.S. and coalition forces would have several key objectives in a peace enforcement or smaller-scale operation, each of which would require certain capabilities:... Establishing and defending zones in which civilians are protected from external attacks."

- "The first priority in defending against a large-scale attack will most often be to neutralize the enemy's offensive capabilities."

- "U.S. military capabilities will be configured to achieve required objectives while minimizing American casualties."

A. DEFEATING THE LAUNCHER BEFORE PROJECTILE IS A THREAT

There exists a need for a Counter-Battery Weapons System (CBWS) to neutralize the enemy's ability to launch large caliber ballistic projectiles at U.S. forces and civilians under U.S. protection. The CBWS needs to be able to determine the launchers position from one in-coming round and surgically destroy that round in as rapid a manner as possible. A secondary purpose that this thesis will not address is eliminating the launcher based on cuing information from the primary system.

The Combat Systems Science and Technology Curriculum at the Naval Postgraduate School has a course sequence designed to solve these kinds of problems and propose system solutions. The class of June 1995, examined the problem solution of defeating projectile by preventing the launch. The class considered this problem to be "shooting the archer" as opposed to "shooting the arrow." A complicated and expensive proposal was developed using acoustic and electromagnetic sensors to detect an initial firing and then a guided projectile to destroy the launcher and nearby personnel

B. DEFEATING THE INCOMING PROJECTILE

This weapon system should have an integrated, multi-unit and autonomous capability to designate the target and automatically engage the threat using a laser tracking beam and a higher power laser destruction beam. Countering the threat from armor, mortars and mobile artillery, the system must be able to respond against projectiles ingressing at up to three km/s from a range of up to 120 km. The response time for incoming projectile detection through battle force threat warning and counterbattery action must therefore be less than 45 seconds. The system should be capable of distinguishing friendly fire from enemy fire through command functions and will also be able to project the most probable impact point of the in-coming round to determine if impact could cause

major damage to friendly forces and to provide warning of imminent danger to ground forces. Projectiles that pose no threat will not be engaged. The initial goal of the CBWS will be to achieve a hard kill of the projectile.

Modern weapon R&D is producing long range over-the-horizon (OTH), high caliber ballistic weapons systems which are small enough to be highly mobile. These weapons systems are being deployed in areas which are becoming an important part of the U.S. military strategy in which Naval forces are being used to support ground forces. The shift from emphasis on open ocean warfighting to the littoral environment as outlined in "Forward...From the Sea" will increasingly place forces at sea within range of these weapons systems. Working with the Marine Corps and their Operational Maneuver From the Sea (OMFTS) warfighting doctrine will require support in various roles. These include: suppression of enemy gunfire, neutralization/denial of enemy operating areas, Naval Gunfire Support (NGFS), interdiction/neutralization of reinforcing elements, and evacuation protection. These capabilities will require execution in day or night, all weather, and OTH scenarios to counter the threat. Specifically, the threat must be engagable in an area 100nm wide and 75nm deep (from an offshore range of 25nm). This must be accomplished with an accuracy of several meters to minimize collateral damage and fratricide. The purpose of the laser weapon system is to provide the capability to achieve these objectives.

Within these requirements, our current inventory of naval gunfire support (NGFS) weapons is inadequate to counter this threat. The technological gains made in other Navy systems has occurred while naval guns have remained virtually unchanged. The maximum range of our most capable system, the 5" 54-caliber M 45, falls far short of the desired ranges and accuracies.

C. ALTERNATIVE SYSTEM SOLUTIONS TO DEFEAT THE LAUNCHER

There are few alternatives to developing this system. One non-material alternative may be to adapt existing counterbattery systems (Firefinder radar) for use by naval forces. Because the precision required to surgically neutralize enemy weapon systems does not presently exist in the Navy's arsenal, improved tactics cannot lead to a solution of the stated problem.

Currently, both the Army and the Marine Corps have ballistic tracking systems in service to locate hostile guns. These again, fall significantly short of the required accuracy and do not address the problem of locating and destroying the incoming projectile. Nevertheless, these systems providing a search capability used in conjunction with a more accurate fire control/targeting system may provide good initial or secondary queuing prior to the terminal phase of the desired weapons system.

Another alternative involves improvements to the Mk 45 projectiles. Several options are being explored including extending the ranges of the projectiles with advanced conventional solid propellants such as liquid propellant or electrothermal chemical propellant. Further improvements to the projectile could provide a "smart" seeker which would aid in the terminal portion of the ballistic trajectory. Use of the existing TOMAHAWK cruise missile as a weapons delivery system would require modifying the missile to be able to target a point defined by latitude and longitude vice using predetermined scene maps and an image matching method. But, again, these systems would do nothing to protect the forces and civilians from the projectile itself.

D. THE SOLUTION APPROACH OF THIS THESIS

The problem can then be summarized as "how it is possible to defeat an incoming ballistic round?" The flowchart below describes the major solution areas and subareas. This thesis is directed

toward solving the problem of deflection/destruction in flight. Specifically, the question "what can be done to change the ballistic projectile's dynamic trajectory?" This is accomplished by examining the forces that control the dynamics and what forces may be applied to change the dynamics (Figure 1).

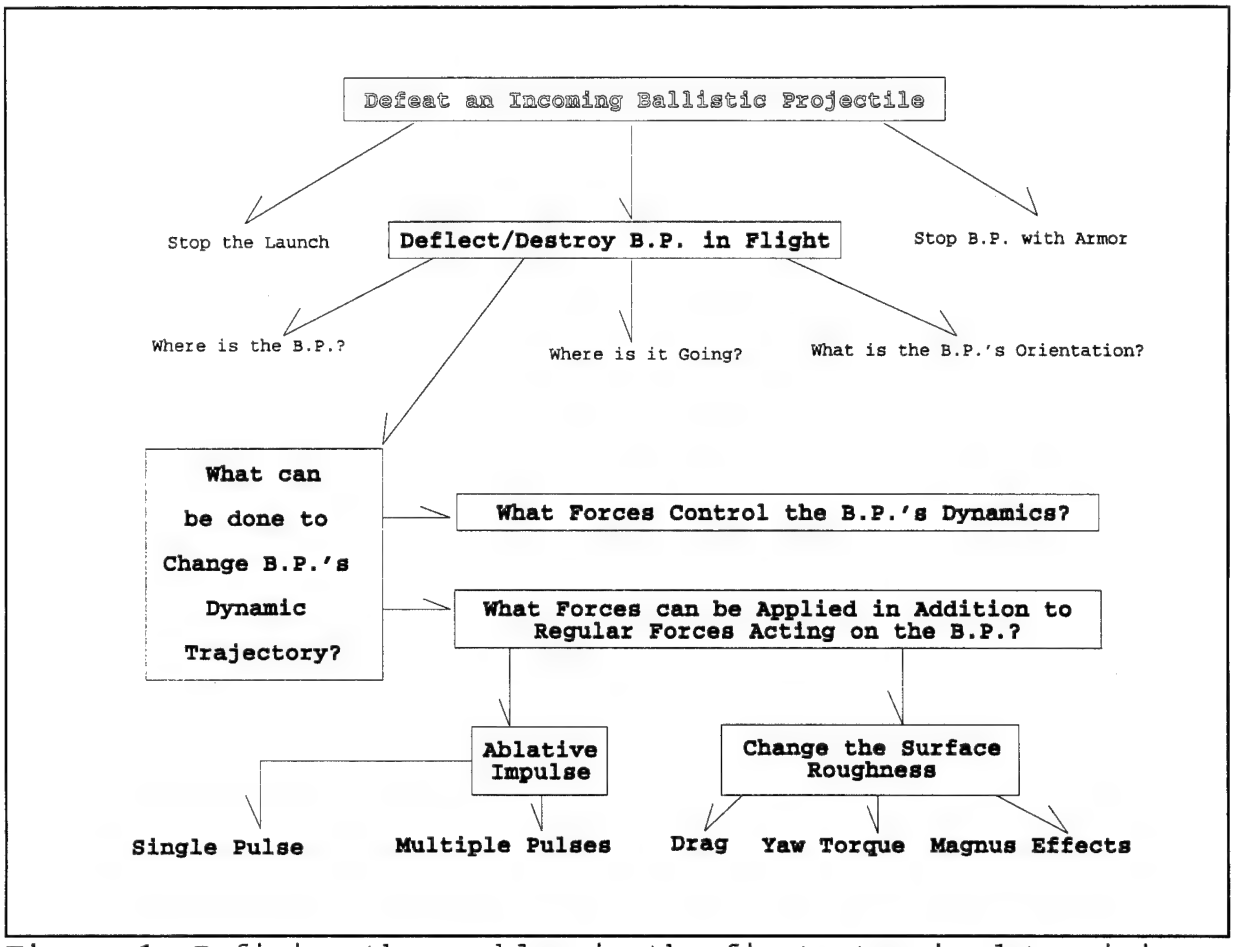

Figure 1 Defining the problem is the first step in determining possible solutions to defeating an incoming ballistic projectile.

The solution of providing armor to defeat the round is considered elementary and could be considered as limiting the scope of the other solutions to larger caliber rounds such as the 155mm. The ability to defeat an incoming round in flight, and ultimately the success of the proposed system, is explored through several theoretical calculations involving laser interaction with the surface of a projectile. Two main areas of research appeared promising in the problem solution: ablative impulse and induced

surface roughness. The impulse problem was handily dismissed due to the large energy requirements. However, the induced surface roughness may have a significant effect on a ballistic projectile's stability and range. This instability desired to deflect the round is most easily obtained by altering the Magnus moment of the projectile. This instability, however, proved to be of insufficient magnitude to defend the projectile's target. The additional drag created by the increased surface roughness appears to be a promising solution.

This thesis estimates the magnitude of effects that could destabilize or reduce the range of a projectile in flight. Most previous work on exterior ballistics has focused on the means for achieving stable flight and maximum aerodynamic efficiency. The magnitude of the effects we seek may demand great pointing accuracy and other laser CBWS problems may arise. These are not addressed here.

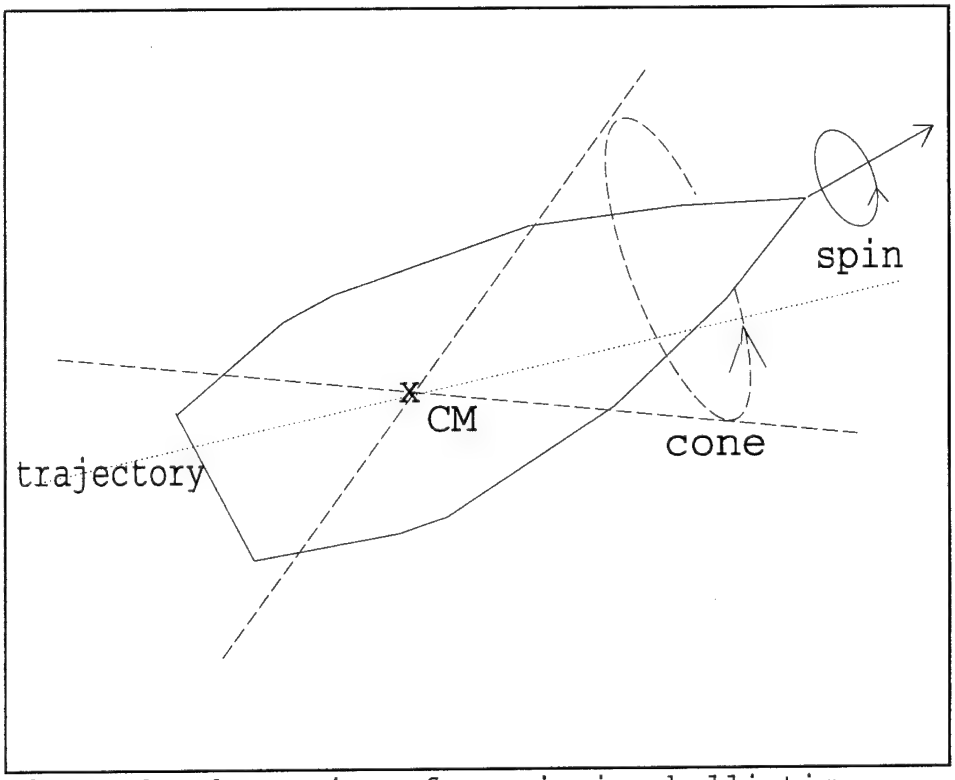

Figure 2 The motion of a spinning ballistic projectile.

The 155mm projectile is used as a model to conduct these calculations because it meets the requirements of a medium to long range artillery threat and is a common weapon in many international forces. The 155mm projectile has many variations of casing design and explosive warheads that are used. The most common projectile is the 155mm HE M107 which is used as a general purpose round by the United States and most other countries that fire the 155mm ballistic projectile. The HE M107 round weighs 95 pounds and is 27.5 inches long. The casing is composed of a medium carbon 4340 steel (a carbon, nickel, monel alloy) that varies in thickness from .25 to .75 inches at the nose.

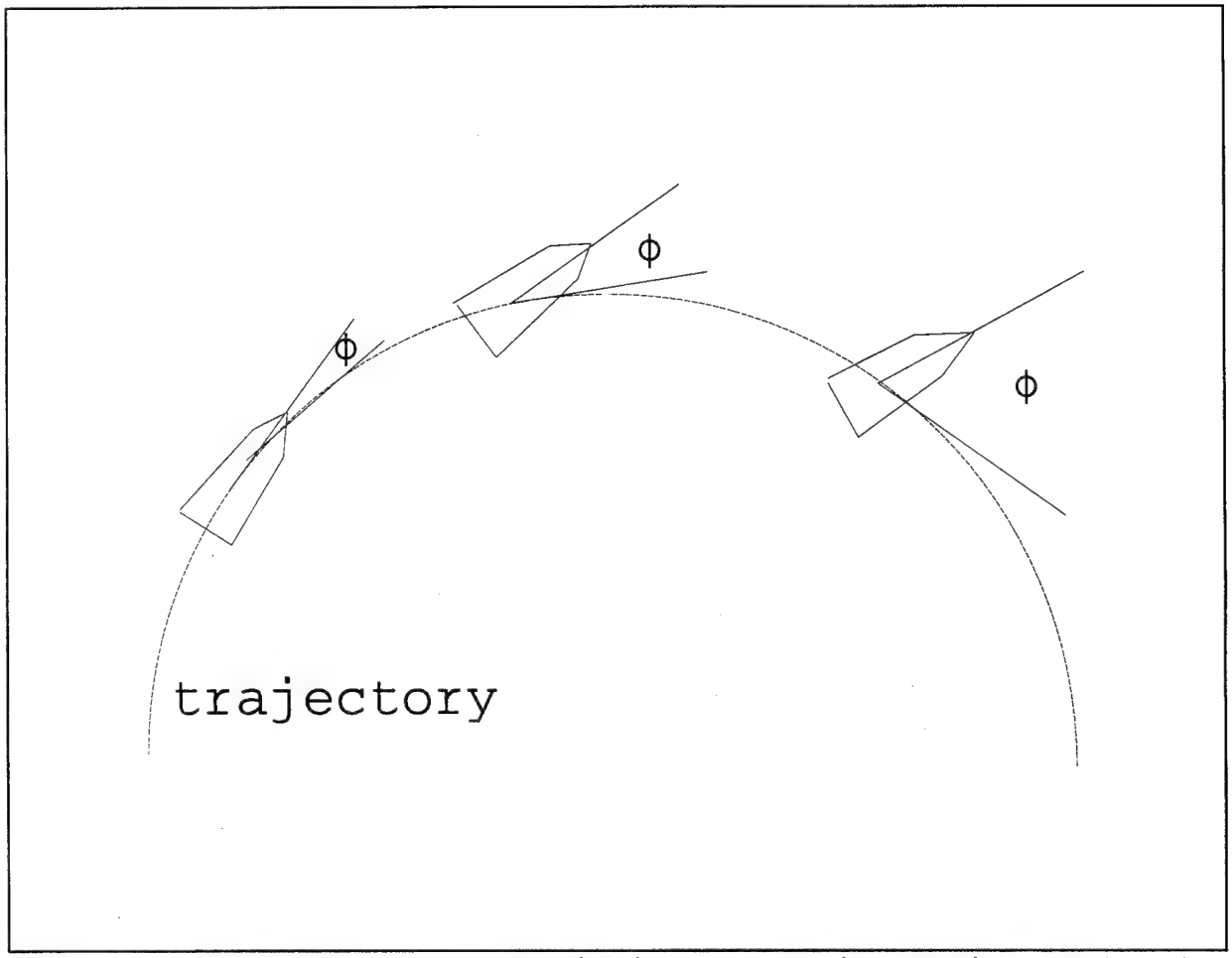

Figure 3 An exaggerated description of the increasing angle of the projectile with respect to the trajectory along the trajectory.

As the projectile travels through the air, it spins at a frequency of 220-250 hz. The spin is imparted by rifling within the bore of the launcher. A variation in the spin rate is due to the differing charges that may be used to fire the projectile. A typical exit velocity of 600 meters/second will be used throughout the calculations. In addition to spin, the ballistic projectile also undergoes a coning motion about the axis of flight with an origin near the center of mass(18.1 inches from the nose tip). The angle of this coning motion is typically 3-5 degrees as the projectile is reaching its apex and then increasing somewhat as the arc of trajectory curves downward toward the target. The coning rate is between 5 and 20 hz.

Ultimately, the system can only be successful if the theoretical results can be further refined and tested experimentally to verify expected system performance. The purpose of this writing is to find possible theoretical means of using laser energy in a CBWS to achieve the national goals stated in the DPG. Specific details of system design will not be addressed.

The thesis will present arguments for five possible mechanisms of achieving a "kill" of the projectile. All of these "kills" will be achieved by deflecting vice destroying the projectile. The first theoretical method discussed to defeat the projectile will be momentum transfer by directed energy impulse. A more complex argument discusses the stability equation for a spinning projectile and addresses the most likely component, the Magnus effect, in relation to achieving instability. Finally, increased aerodynamic drag is examined as the most likely means to achieve a successful engagement against an incoming spinning ballistic projectile.

II. IMPULSE DELIVERED BY LASER INTERACTION

A. LASER EQUATIONS AND IMPULSE THEORY

Before examining any calculations of ablative impulse, it is necessary to introduce the equations which will be used. The equations that will be used were developed in class notes used at the Naval Postgraduate School for various courses examining directed energy capabilities (Schriempf, 1974). The terms that will be used are defined below:

$F_o = (1 - \Re) I$ The laser power density absorbed where $\Re$ is the Reflectance, I is the laser power density arriving at the surface and F_o is the power transmitted through the surface per unit area.

τ_p The pulse length (duration).

D_p The thermal diffusion length is the distance required for the temperature to drop $1/e$ of the surface value.

ρ The material density.

T_0 The initial temperature.

T_m The melting temperature.

T_V The vaporization temperature.

C_s, C_l The specific heat of the solid, liquid.

L_m, L_v The latent heat of melting, vaporization.

T_b The boiling temperature.

$\kappa = \frac{K}{\rho} C$ The thermal diffusivity is equal to the product of the thermal conductivity and the specific heat divided by the density.

The criterion for vaporization of a diffusion thickness is given by:

$$F_o \frac{\tau_p}{D_p} \geq \rho \left[C_s (T_m - T_o) + L_m + C_l (T_b - T_m) + L_v\right]. \qquad (2.1)$$

When numerical values are inserted, the L_v term dominates the equation simplifying to the form:

$$F_o \frac{\tau_p}{D_p} \geq \rho L_v. \qquad (2.2)$$

Since, $D_p \approx 2\sqrt{(\kappa \tau_p)}$, this then becomes:

$$F_o \geq 2 \frac{\sqrt{\kappa}}{\sqrt{\tau_p}} L_v \rho. \qquad (2.3)$$

Solving this equation for the pulse length gives:

$$\tau_p > 4 \kappa \frac{L_v^2}{F_o^2} \rho^2. \qquad (2.4)$$

Now to solve the specific impulse on a target will require several assumptions before this can be carried any further.

1) The beam radius, R, is much larger than the diffusion length.

2) The target is very thick compared to the diffusion length.

3) The melting will be ignored.

The time for the surface to reach vaporization temperature is:

$$\tau_b = \frac{\pi}{4} K_s \rho C_s \frac{T_v^2}{F_o^2} . \qquad (2.5)$$

The surface erosion speed is taken from equation 2.1 substituting Δz for the diffusion length. This represents the thickness of the material evaporated during a time Δt. The erosion speed is then expressed as:

$$U_s \equiv \frac{\Delta z}{\Delta t} = \frac{F_o}{\rho} 1/[C_s(T_m - T_o) + C_p(T_v - T_m) + L_v] . \qquad (2.6)$$

Since $L_m \ll L_v$; $C_l \approx C_s = C$, then $U_s \approx \frac{F_0}{\rho} 1/[L_v + CT_v]$. (2.7)

The vapor blow-off speed is derived from the momentum conservation, $\rho_v U_v = \rho_s U_s$, resulting in:

$$\rho_v U_v = F_o/(L_v + C T_v) . \qquad (2.8)$$

The associated pressure with the blow-off is then:

$$P = \rho_v U_v^2 = \rho_v \frac{R}{M} (\textit{gas constant/molecular weight})\, T_v \quad \textit{so,} \quad U_v = \frac{\sqrt{R}}{\sqrt{M}} \sqrt{T_v}$$

and combining this with equation 2.8 results in:

$$P = F_o \frac{\sqrt{R}}{\sqrt{M}} \sqrt{T_v}/(L_v + CT_v) \approx F_o \sqrt{C} \sqrt{T_v}/[\sqrt{3}(L_v + CT_v)] \qquad (2.9)$$

since $C \approx 3\frac{R}{M}$ for most metals.

Now, the specific impulse delivered during an energy pulse is:

$$I_m = P\,(\tau_p - \tau_b)\,. \qquad (2.10)$$

Substituting equations 2.5 and 2.9 into 2.10 and using typical values results in a simplified form:

$$I_m = 8\,E_o\left(1 - 6\,\frac{\tau_p}{E_o^2}\right), \quad [(taps)\ dyn{\cdot}s/cm^2] \qquad (2.11)$$

where E_o is the pulse energy per unit area (fluence) $= F_o\tau_p$, T_p *units are* μs.

This equation will generally result in agreement with experimental data within a factor of two. This is sufficient for the estimates of this thesis. If the results of further calculations indicate a possible effect within a factor of two from current technology, then better estimates would be in order.

One additional aspect of laser theory should be addressed here. If the E_o is very large, the delivered impulse will fall off with increasing values of E_o. This is due to the absorption of laser energy within the vapor near the surface of the target. At some value of power density, the plume of vaporized material blow-off from the target will become hot enough that the surrounding air or vapor are sufficiently ionized to absorb large amounts of the laser radiation. This phenomenon is called laser absorption.

Another problem is called beam decoupling. When the laser beam electron density increases to a value where the plasma frequency is larger than the laser frequency, then the light interaction with the free electrons dominates. The laser is cut-off from the surface.

With these in mind, it is important to find the critical energy density at which these processes occur. The upper limit density is about 10^{23} electrons per cubic cm electron density where the material reaches a temperature of full ionization. But, this is not accurate enough since the ionization degree is very

sensitive to the temperature. Figure 4 shows the predictions for the impulse as a function of the pulse energy (Nielsen, 1972). These values will be used later in the calculations for ablative impulse.

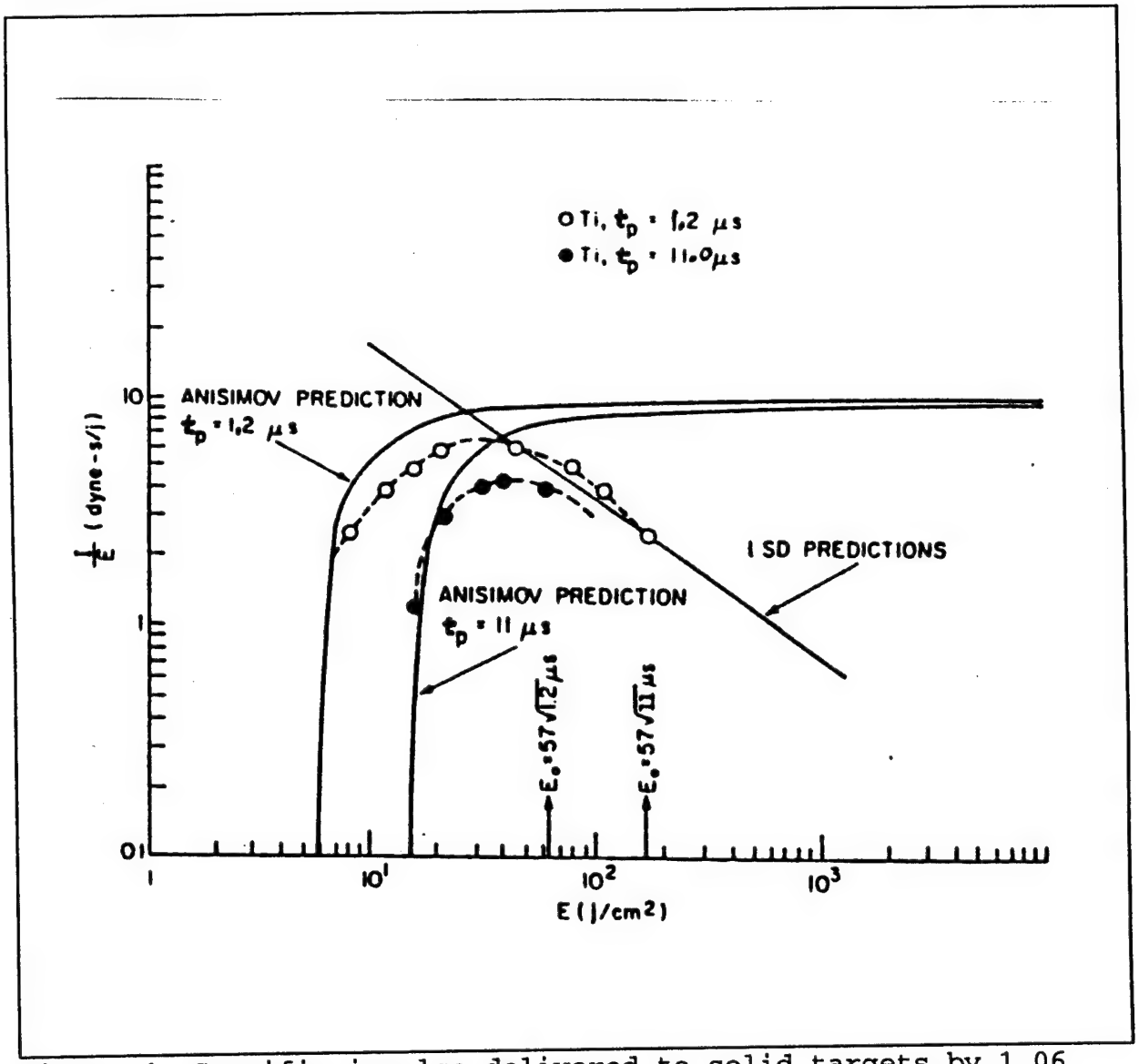

Figure 4 Specific impulse delivered to solid targets by 1.06 micron laser radiation (Nielsen, 1972).

B. ABLATIVE IMPULSE CALCULATIONS

1. Single Pulse Impulse

The impulse calculations are examined first since this would be the easiest and most direct method of deflecting an incoming round. A Laser induced ablation from a single pulse would be the preferred method of destruction if it were physically possible. This would require a less sophisticated system that could "fire and forget." The problem is complicated when a system is required to accurately track and reengage a target multiple times. This requirement also detracts from the ability to rapidly engage the next subsequent target in a dense battlefield. With this in mind, and using the equations for critical energy of a laser system, it is possible to determine the feasibility of the single pulse system.

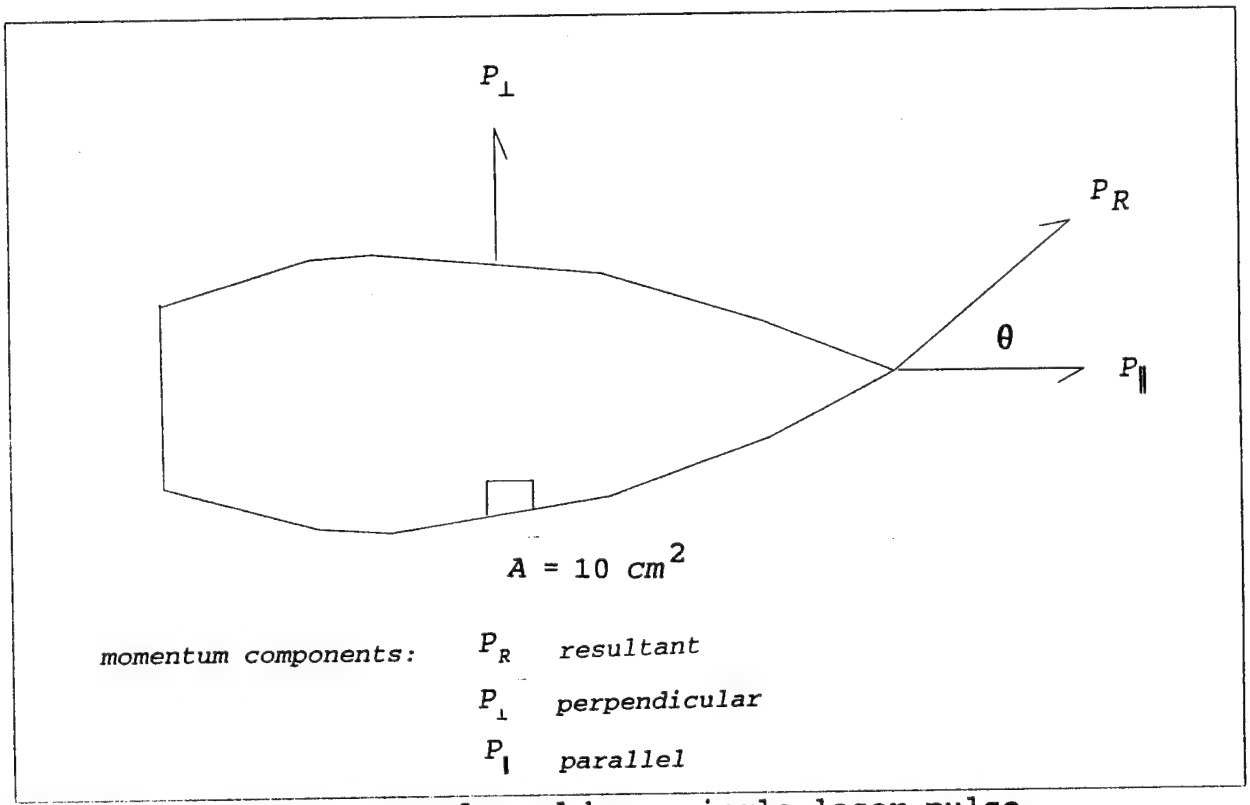

Figure 5 Impulse transferred by a single laser pulse.

To further simplify the initial calculation, a perpendicular impulse will be assumed. If the required energy is at physically attainable levels, then further calculations for reduced angle impulse will be in order.

The impulse transferred by ablation is found by equation 2.12 to be proportional to E_o for $\tau_p \leq 10\mu s$ and $E_o > 20 J/cm^2$ when the term in the bracket becomes small compared to one:

$$I_m \cong 8E_o\left(1-\left(6\frac{\tau_p}{E_o^2}\right)\right). \qquad (2.12)$$

The impulse is calculated from the change in momentum required where the momentum of the moving projectile is,

$$p=mv=1.8x10^9 gcm/s. \qquad (2.13)$$

For a single pulse system, a shipboard close-in defense would require a deflection on the order of 50 meters for every 1000 meters traveled by the projectile. The result would be a .05 rad change in direction or a change in momentum of

$$(\Delta p)_{reqd}=.05(1.8x10^9)=10^8 gcm/s. \qquad (2.14)$$

Then, the impulse transferred in a 10 square cm area to the projectile is estimated by:

$$(I_m)_{reqd}=\frac{(\Delta p)_{reqd}}{A}=10^7 dyns/cm^2. \qquad (2.15)$$

Finally, referring to equation 2.12, the energy fluence required will be $10^6 J/cm^2$ with a pulse duration of 10^{-6} seconds Presently, this is not within the realm of possibilities for current laser

systems. Therefore, further calculations of reduced angle impulse are not required. However, there is another way to examine the problem. It may not be a close-in defense system that is engaging the target projectile. Without placing any limitations on the amount of deflection required for a given length of travel, a calculation may be conducted for a change of yaw angle. A significant change of yaw angle of about 10-20 degrees would change the drag significantly and alter the range of the projectile. Using a spinning top approach and a small angle change, a first approximation again rules out the possibility of sufficient energy for a single pulse.

From Figure 4, values of Energy $30\ J/cm^2$ and I/E of 5 $dyn\ s/J$ show that an impulse of $150\ dyn\,s/cm^2$ could be attained.

To determine the required impulse, one finds the required torque from the required change in angular momentum in the following steps:

the torque, $\mathbf{T}=F\cdot a$, (2.16)

the moment of inertia, $\vec{I} = \frac{1}{2}MR^2$, (2.17)

and the angular momentum, $\vec{L} = \vec{I}\omega = I\omega\cdot\hat{n}$ (2.18)

so that, $\frac{d\vec{L}}{dt} = \mathbf{T}$. (2.19)

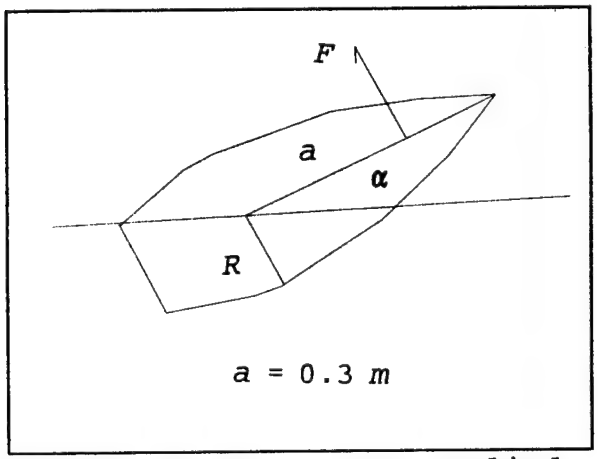

Figure 6a The torque applied.

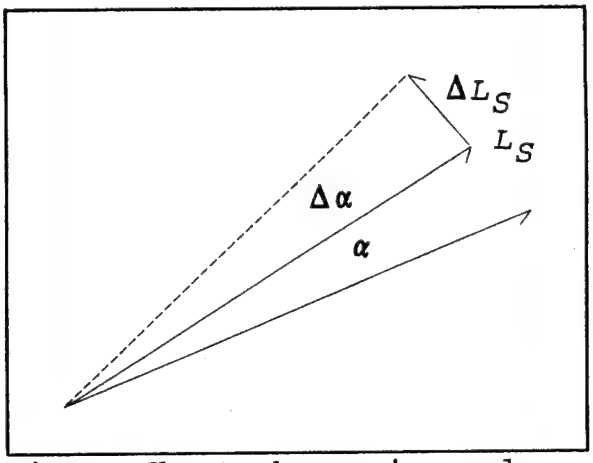

Figure 6b A change in angle.

Therefore, the torque can be expressed as:

$$\frac{d\vec{L}}{dt} = I\omega\frac{d\hat{n}}{dt} = I\omega\frac{d\alpha}{dt} = F\cdot a. \qquad (2.20)$$

The impulse per unit area required is:

$$Imp_{req} = \frac{F\cdot\Delta t}{A} = \frac{I\omega}{a\cdot A}\Delta t\frac{d\alpha}{dt} \approx \frac{I\omega}{aA}\cdot\Delta\alpha. \qquad (2.21)$$

Using the values from Figure 4, $E_{crit} = \frac{Imp_{req}}{5}$ with the result of 30 MW. This is an energy fluence far beyond the laser absorption threshold and is an implausible solution with current technology.

2. Multiple Pulse Impulse

This leaves the less desirable option of impulse delivered by multiple pulses to be examined. Using the results of equation 2.21, the total energy required must be divided into optimal energy pulses. If $E_{opt} = 30\frac{J}{cm^2}$, then 10^5 pulses are required. Using 10 *ps* pulses at optimal energy, it is possible to determine how much engagement time is possible as the projectile cones. The engagement time is estimated by the following using a coning rate of *5 Hz*:

$$\omega_c = 2\frac{\pi}{5}Hz \; also \; v = R_c\omega_c = a\tan\alpha\,\omega_c. \qquad (2.22)$$

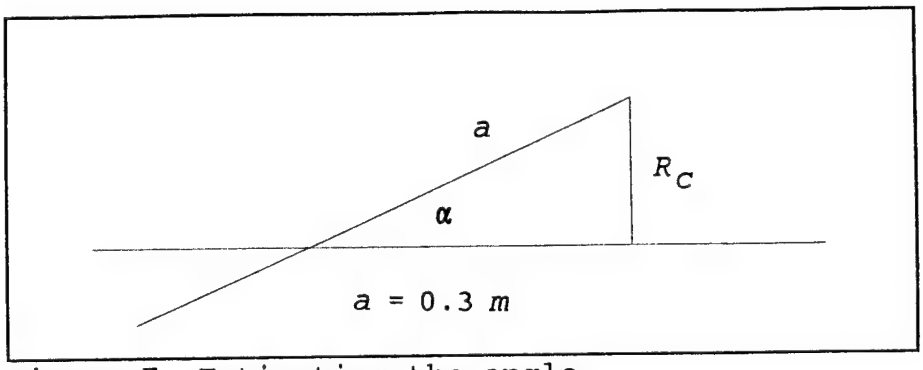

Figure 7 Estimating the angle.

With the established coning rate and angular velocity, an engagement can only be achieved within a period of .06 seconds. Applying these pulses over the engagement time for a 1 ns pulse results in a power requirement of $6x10^{10}$ Watts which is still well outside of an expected capability.

The impulse calculations demonstrate that it is currently not possible to achieve a "kill" on a ballistic projectile with the ablation energy transfer alone. The next step is to determine how the stability may be affected by changing the aerodynamic forces acting on the projectile.

III. STABILITY

There are several topics that should be explored before beginning the calculations to prove or disprove that a viable CBWS can cause instability. Most importantly, a sound understanding of spinning projectile stability theory is established as a framework. Then, using the stability as a guideline, one term (the Magnus moment) in the final stability equation appears to be most promising for further analysis in causing instability. The Magnus force and ultimately Magnus moment must be defined and discussed to determine whether these components are worthy of further calculations to support an instability argument.

The conditions for stability of a spinning ballistic projectile are given by McShane et al. The following discussion is a summary of the results of this analysis with the details given in Appendix A.

A. THE EQUATIONS OF MOTION

The focus of this analysis is the derivation of the equation of motion of the yawing motion due to the various aerodynamic forces acting on the projectile. The velocity vector, $\vec{u}$, of the projectile with respect to the ground can be decomposed into a component along the projectile axis of symmetry, u_1, and a complex component, $\xi = u_2 + iu_3$, where u_2 and u_3 are the velocity components perpendicular to the projectile axis in a coordinate system fixed to the projectile. The tangential velocity of the center of mass is U. The ratio, $\frac{\xi}{U}$, is the "vector of yaw" which has the magnitude of $\sin\delta$. A new variable is defined as:

$$\lambda \equiv \frac{\xi}{U} e^{i\int_0^P \nu \, dp}, \qquad (3.1)$$

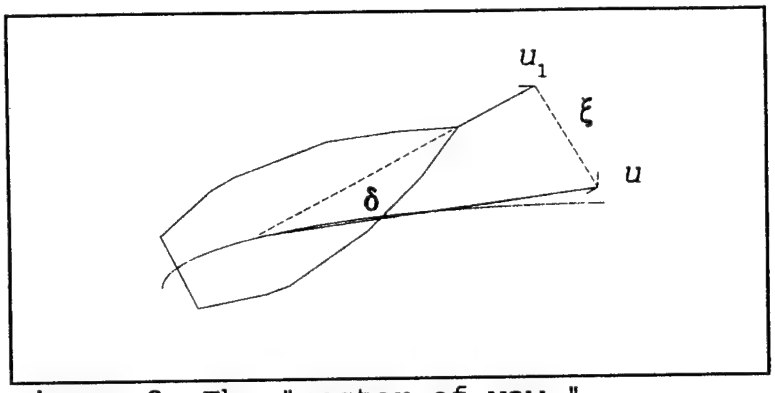

Figure 8 The "vector of yaw."

where P is the arclength along the trajectory in calibers and ν is the spin rate per caliber of travel. The yawing equation of motion derived in Appendix A is a second order inhomogeneous differential equation for the quantity, λ.

The solutions to the homogeneous equation are given as exponential functions in P as:

$$\lambda = \sqrt{\frac{\sigma_o}{\sigma}} e^{\frac{1}{2}\int_0^P [(J_D - J_N - k^{-2}J_H + J_A \frac{md^2}{A}) \pm (J_N - J_D - k^{-2}J_H - (2J_T - J_A)\frac{md^2}{A})/\sigma + i\nu A(1\pm\sigma)/B]\, dp}, \qquad (3.2)$$

where the integrand is a function of the relevant aerodynamic force coefficients. The yawing motion is then given by the superposition of the two solutions of the homogeneous equation plus a particular solution of the inhomogeneous equation:

$$\lambda = L_1\lambda_1 + L_2\lambda_2 + \lambda_p. \qquad (3.3)$$

The coefficients L_1, L_2 would be determined by the initial yaw and rate of yaw on the trajectory.

The projectile is stable along the trajectory if the solutions

λ_1 and λ_2 decrease in magnitude so that in the limit of long trajectory, only the particular solution remains. This means that λ is independent of the initial conditions. The particular solution need not be small however. For large spin, the rate of precession and the direction of its axis changes only slowly. As the trajectory curves, the yaw for a stable projectile can still be significant. In fact, the projectile becomes more stable along the trajectory as the velocity of the projectile slows at a greater rate than the spin.

In reality, the yaw will be small if the projectile is stable and the solution of the particular integral is small; this is almost always the case unless high-angle fire is used, then the particular solution may not be small.

The analysis of stability of the yaw motion concentrates then on the two solutions λ_1 and λ_2 which can be written in the form:

$$\lambda_{1,2} = e^{\int_0^P [\frac{1}{2}(a_1+a_4-\frac{r'}{r}) \pm r]\, dp}, \qquad (3.4)$$

where a_1, a_4, r are functions of the aerodynamic coefficients (defined in Appendix A) and the spin rate which is not time independent along the trajectory.

One can see that the yaw will decrease if and only if the real part of the first bracket under the integral is negative and in absolute value greater than the real part of the second.

In the following, we will summarize this analysis with the thought in mind to determine which of the aerodynamic coefficients must be changed by laser action, for instance, and by what magnitude in order to destabilize the projectile.

B. THE STABILITY EQUATIONS

The purpose of this section can be achieved now by defining the terms of stability which are derived more thoroughly in the appendix. The stability factor S and the stability terms are usually expressed as:

$$\frac{1}{S} \equiv \frac{4B^2k^{-2}J_M}{A^2\nu^2},$$

$$S_1 = J_N + k^{-2}J_H - J_D - J_A\frac{md^2}{A}, \tag{3.5}$$

$$S_2 = 2J_N - 2J_D - 2J_T\frac{md^2}{A}, \text{ and}$$

$$S_3 = 2k^{-2}J_H + (2J_T - 2J_A)\frac{md^2}{A}.$$

The conditions for stability are expressed as the inequalities:

$$\frac{1}{S} < \frac{S_2S_3}{S_1^2} \qquad \text{and} \qquad S_1 > 0. \tag{3.6}$$

It is worth noting that the spin term, ν, appears only on one side of the inequality. This is useful for determining the effect of varying spin rate on a projectile's stability.

These inequalities yield the desired framework for comments on projectile stability. Namely, there are conditions which do not satisfy the inequalities that are cause for instability. When either of the terms of equation 3.6 become negative, the conditions for stability are violated. These are the conditions for exploitation in the calculations. It becomes clear in analysis

(see the discussion at the end of Appendix A) that the only term which can be reasonable exploited to cause instability without catastrophic damage to the entire projectile is the Magnus moment term, J_T. This is true because this term has a polarizing effect on the first condition of 3.6. Since this term contains opposite signs in each term of the numerator, then it will have an effect in opposite directions of the over-all stability. Further, because the Magnus coefficient can either be positive or negative depending on its relation to the center of mass location, it can change signs within each term (but, change them both in opposite directions simultaneously).

The drag term also appears capable of causing a change in the stability term, S_2, since it is of the same order of magnitude as the Magnus term. However, the J_N term contains the drag coefficient as well. So a change in the drag will result in a corresponding change in J_N, nullifying any effect it would have on the stability. In examining equations 3.5, it can be seen that increasing the drag will cancel out a similar increase in J_N. Applying any change in the drag term to either the denominator or the numerator of equation 3.6 will result in similar cancelling of the effect. This leaves the Magnus term as the only term that can be altered in such a way to violate the stability criteria expressed in equation 3.6.

C. THE MAGNUS FORCE AND MAGNUS MOMENT

The Magnus moment is the most likely component of stability to be exploited. By increasing the Magnus effect sufficiently, one can cause instability. Before making the argument for instability, it is appropriate at this point to discuss the Magnus force and Magnus moment.

First, the coordinate system of the projectile should be established. The vector components of this system will be used to define the Magnus terms. A ground-based, right-handed coordinate system will be used with a center of mass of the rigid projectile serving as the origin.

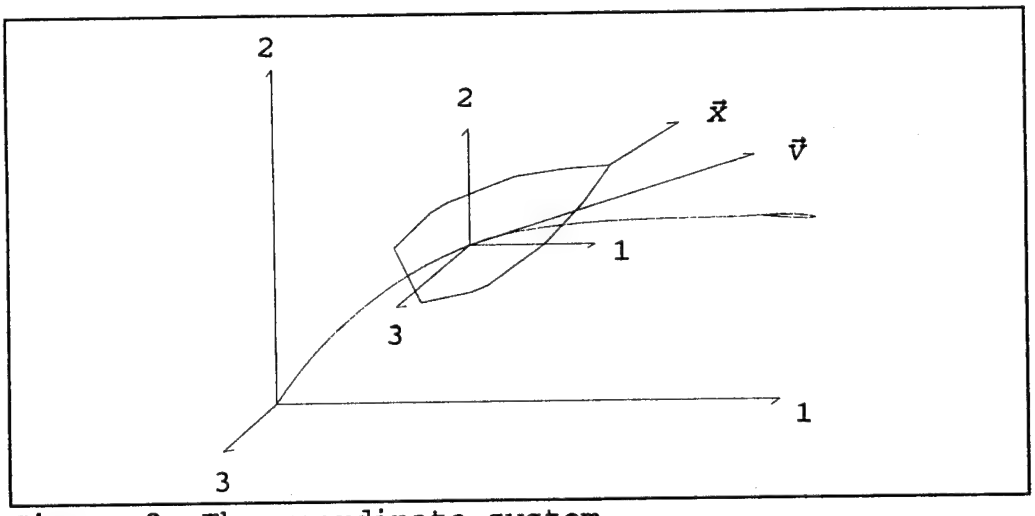

Figure 9 The coordinate system.

The projectile is considered a solid body of revolution. Along the axis of rotational symmetry, a unit vector $\vec{x}$ is chosen positive in the direction toward the nose from the center of mass. Therefore the total angular momentum of the body can be expressed as the sum of:

1) the angular momentum about $\vec{x}$

and the

2) total angular momentum about an axis perpendicular to $\vec{x}$.

Both vectors are in the ground-fixed coordinate system.

The sum of all the forces and moments will determine the position of the projectile. For this discussion, however, only the notation that is necessary to understand the Magnus contributions will be introduced including several additional variables that provide an understanding of this effect.

For the angular momentum about $\vec{x}$, the magnitude of the product AN, where A is the moment of inertia of the body about $\vec{x}$, and N is the axial spin (angular velocity with a positive direction of a

right-handed screw about $\vec{x}$ expressed in radians per second) result in the total angular momentum represented by the vector $AN\vec{x}$.

An aerodynamic force or moment (torque) is produced by the interaction of the rigid body and the fluid of the atmosphere around it. There are several in addition to the Magnus components that are considered necessary to form a complete model of symmetrically spinning projectile behavior. These are outlined in Appendix A. The drag force will be introduced in more detail in a later chapter as a model for examining the effect of a roughened projectile skin on an aerodynamic coefficient.

The Magnus effects on spinning projectiles were first documented by G. Magnus in the 1800's. He observed that a spinning musket shot experienced drift in the direction of spin as if there were an additional sideforce acting on the projectile. It has been consistently recognized that this effect is an important contribution in determining stability and trajectory of spinning projectiles, missiles and bombs. Although there has been a great deal of interest in these effects, there are few studies that examine these effects in great detail. Because of the complexity of this effect we will at this stage use the basic principle of the Magnus force and Magnus moment as outlined below make a simple estimate of the effect of varying surface roughness. To date, there have been no models developed to describe the complexities of an asymmetric flow caused by an asymmetric body, although one paper addresses the non-linear effects of the Magnus force for large yaw (Platou, 1956).

It is widely accepted that the Magnus effect is produced entirely by viscous effects. An asymmetric boundary layer (around a symmetric rigid body) is produced by both the spin of the projectile and its angle of attack. Most of the research to date has examined bodies with low angles of attack and very smooth surfaces. A simple illustration shows the asymmetric boundary layer and the resulting forces for the low angle of attack.

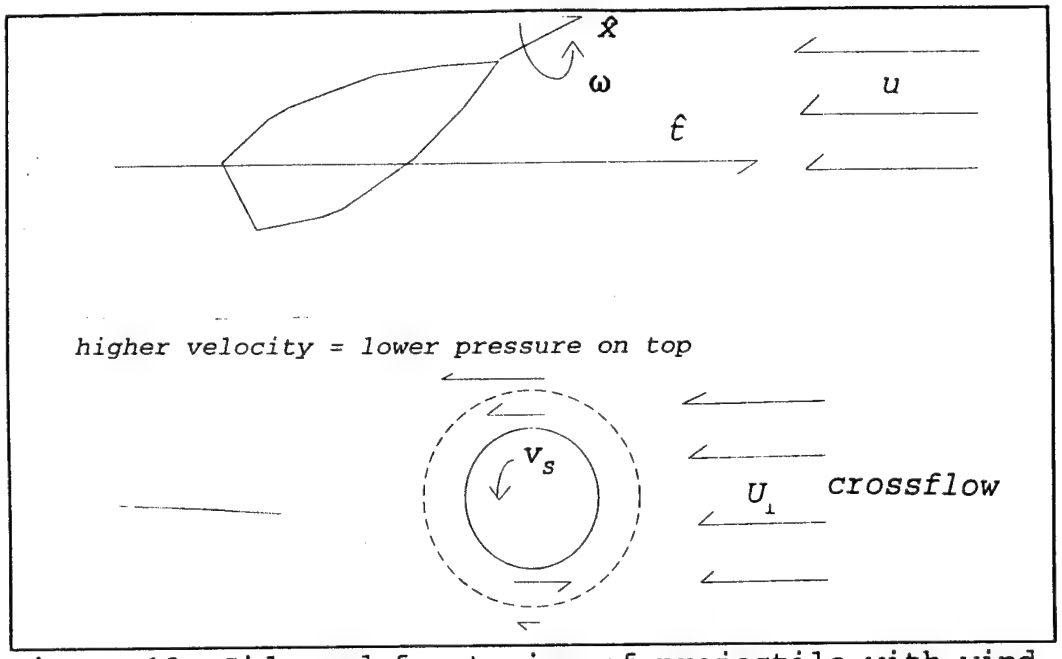

Figure 10 Side and front view of projectile with wind.

In Figure 10, we consider a cross section through the projectile with its plane spanned by the trajectory and the direction given by $\hat{t} \times \hat{x}$, where $\hat{t}$ is the vector along the trajectory. The bottom view represents the projectile cross section in this plane with a boundary layer and the cross velocity component of the wind as it adds or subtracts to the boundary layer velocity due to the projectile spin in this plane.

On the upper portion of the cross section, the fluid flow over the projectile is parallel to the rotational motion, and on the lower side they are in opposite directions. On the upper side, the mean velocity in the boundary layer is larger than on the lower side. Therefore, the pressure is larger on the lower side and the effect is a net pressure force acting upward in the Figure. The projectile is acted upon by a net force to the left when viewed along the trajectory.

For a large angle of attack (large yaw in excess of 20 degrees), the boundary layer begins to separate and vortices flow into the outer inviscid flow. The result is an equal and opposite circulation causing an additional sideforce. Currently three dimensional models of boundary layer behavior are too difficult for

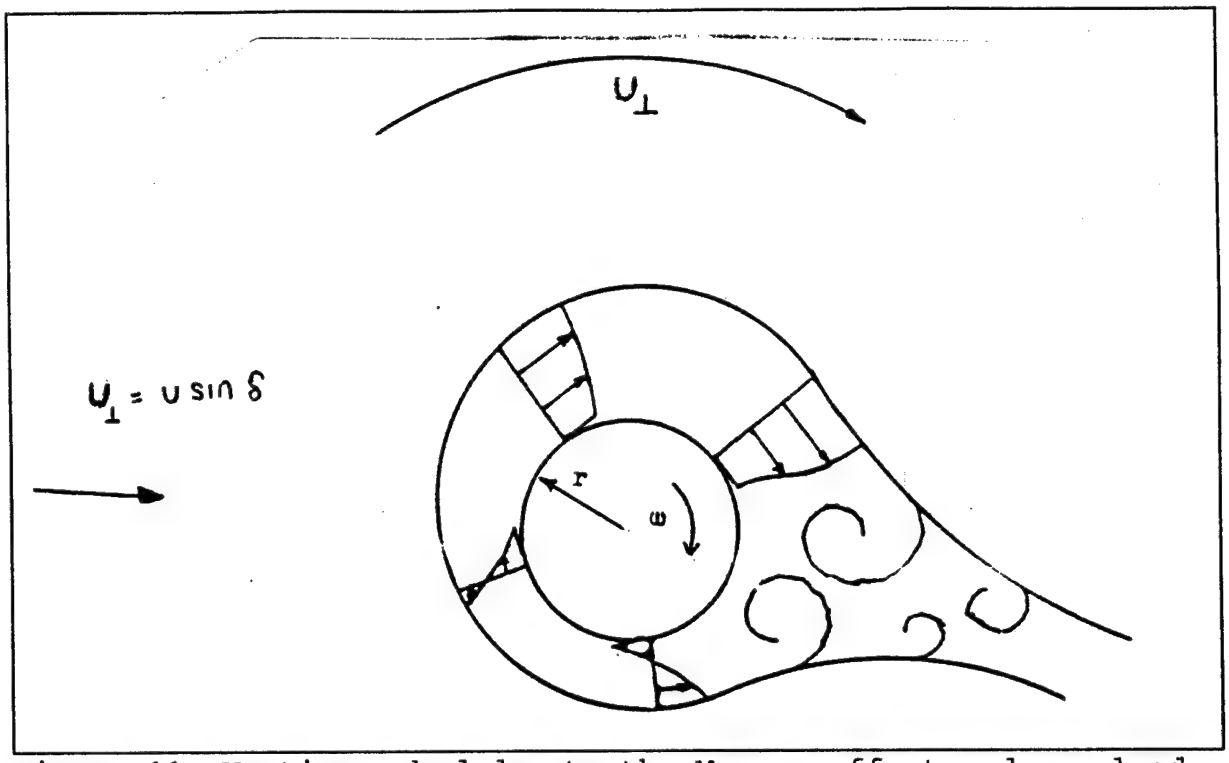

Figure 11 Vortices shed due to the Magnus effect and may lead to additional force component in the Magnus terms (Power, 1974).

theoretical predictions beyond the crudest approximations.

Since the effects on the 155mm projectile are calculable within a low angle of attack, the further analysis of the three dimensional boundary layer are not conducted in this work. Such circulation and vortex shedding may contribute to rapid growth of instability as precession occurs and should be further investigated in subsequent work.

For the symmetric body before a laser has induced surface roughness, the Magnus force can be fairly accurately described. The Magnus force is the result of the fluid interaction of the air stream flowing over the boundary layer of a yawed spinning body. The magnitude of the force is $\rho d^3 K_F N v \sin\delta$, *where* K_F is the dimensionless coefficient of the Magnus force. The force is perpendicular to the yaw plane. The Magnus force is represented by the vector $\vec{x}\times\vec{v}$ for positive values of N. The result is illustrated in Figure 12.

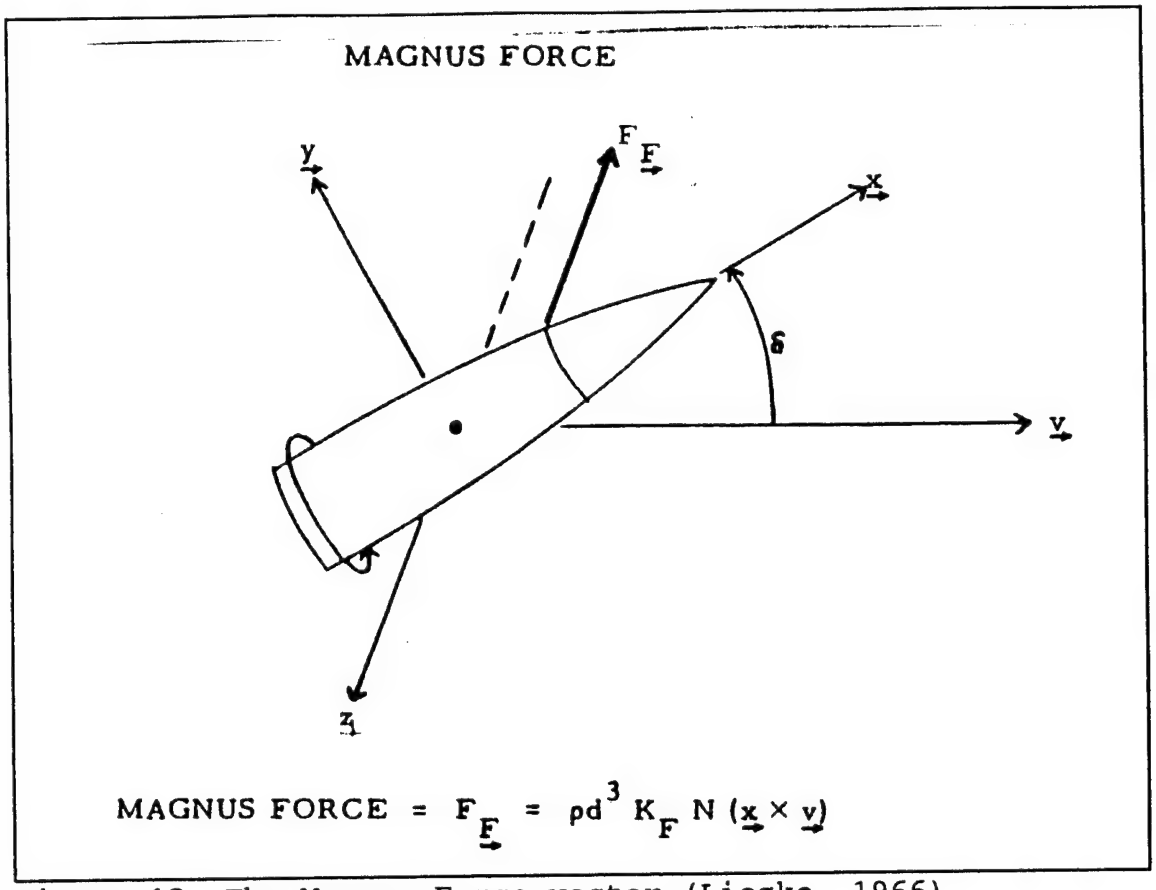

Figure 12 The Magnus Force vector (Lieske, 1966).

Some research has been conducted to determine the value of the coefficient and relates it to the length to diameter (L/D) ratio of the body for low angle of attack and very smooth surfaces in supersonic flight (Power, 1974). Since we are trying to determine the effect of varying the roughness, this solution is not helpful in the end, but may be used to determine a ballpark value of the unperturbed coefficient. The results of this research are reproduced in the figure on the following page.

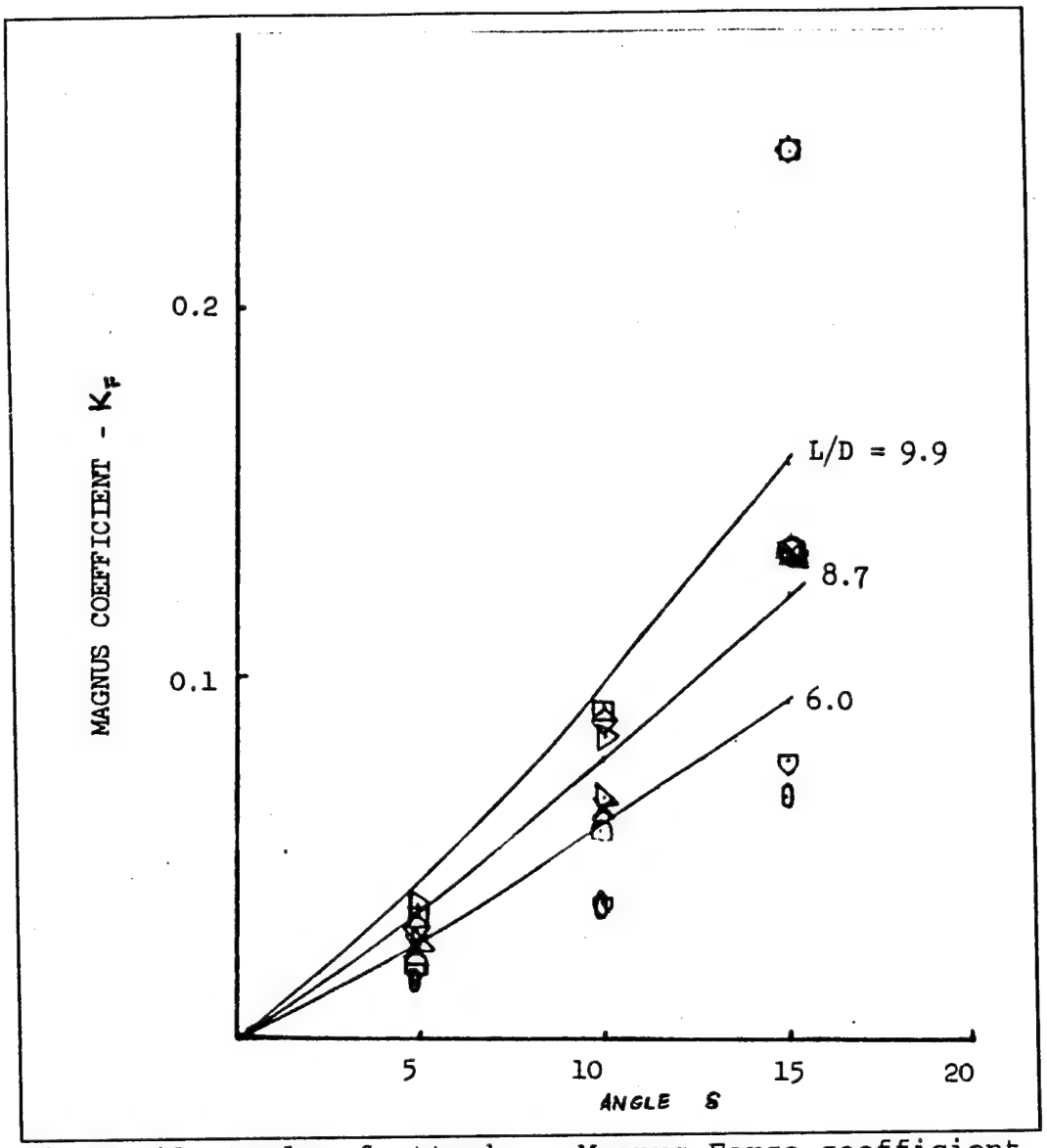

Figure 13 Angle of attack vs Magnus Force coefficient (Power, 1974).

Although it is the Magnus force that results from the roughness that we hope will ultimately cause instability, it is the moment arm placement of this force on the body that causes the torque about the center of mass. This is the contribution of the Magnus moment. If the Magnus force does not pass directly through the center of mass of the projectile, then a resulting Magnus moment is produced. The magnitude of the moment is given as is

the dimensionless coefficient of the moment. This coefficient is approximated in McShane, et al. with a dependence upon the center of mass location in the projectile (the location of the *CM* is on the horizontal axis of Figure 14) (McShane, 1953).

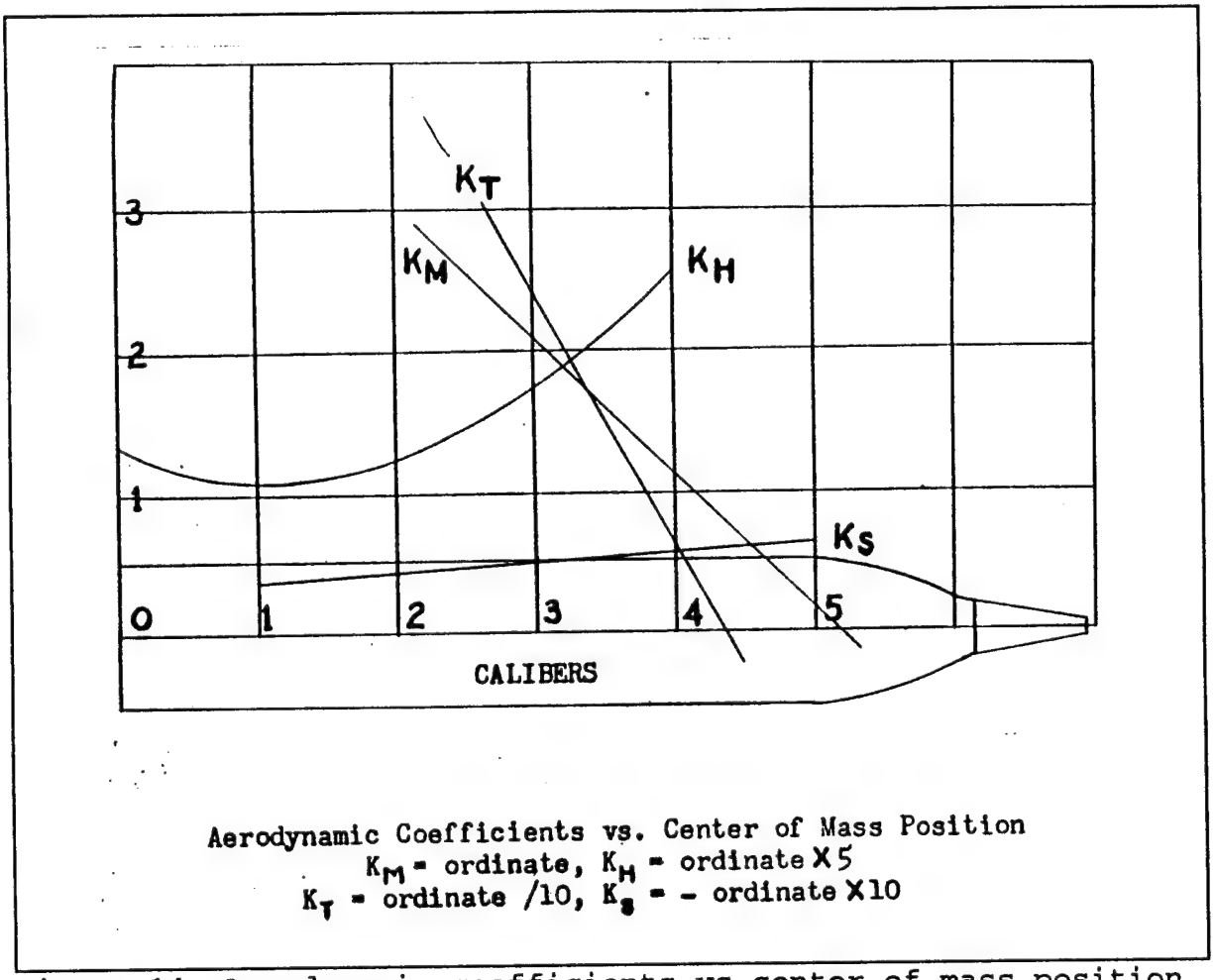

Figure 14 Aerodynamic coefficients vs center of mass position (McShane, 1954).

The Figure depicts firing data obtained for a 4.5 inch rocket and although not precise for our purposes, it provides a general idea of how the magnitude of the coefficients varies. The value of the coefficient is read from the graph at the point where the moments are applied in relation to the center of mass position). For the 155mm projectile, the center of mass would be near the number two on the axis of Figure 14. This gives a general idea of

representative values for the Magnus moment if a Magnus force were applied to the forward third of the projectile (e.g. a Magnus force applied at position 4.5 would yield a Magnus moment coefficient near zero).

The value of the moment coefficient may be positive or negative as the mean position of the force moves away from or toward the center of mass. The hope is to achieve a roughness that will produce a force with a different length moment arm from the center of mass and thus produce a change in the Magnus moment coefficient. The actual center of mass will not have changed, but the position of the Magnus force relative to the center of mass will have the effect of changing the center of mass for predicting the Magnus moment coefficient with the above Figure. The Magnus moment lies in the yaw plane and is perpendicular to $\vec{x}$. The vector $[\vec{x}\times(\vec{x}\times\vec{v})]$ has magnitude $v\sin\delta$. The moment is depicted and expressed in Figure 15.

It is hoped that inducing a Magnus moment by increasing surface roughness would become a technologically feasible possibility. If it becomes possible to use surgical precision (to within centimeters) to produce a roughness at a desired location from the center of mass, then the resulting torque would be changed by the amount r X F, where r is the distance from the center of mass and F is the magnitude of the Magnus force. Ultimately, then the problem of defeating an incoming projectile could be achieved with a calculated amount of energy directed toward a specific point on the projectile with predictable results. This would be the most efficient use of the proposed system.

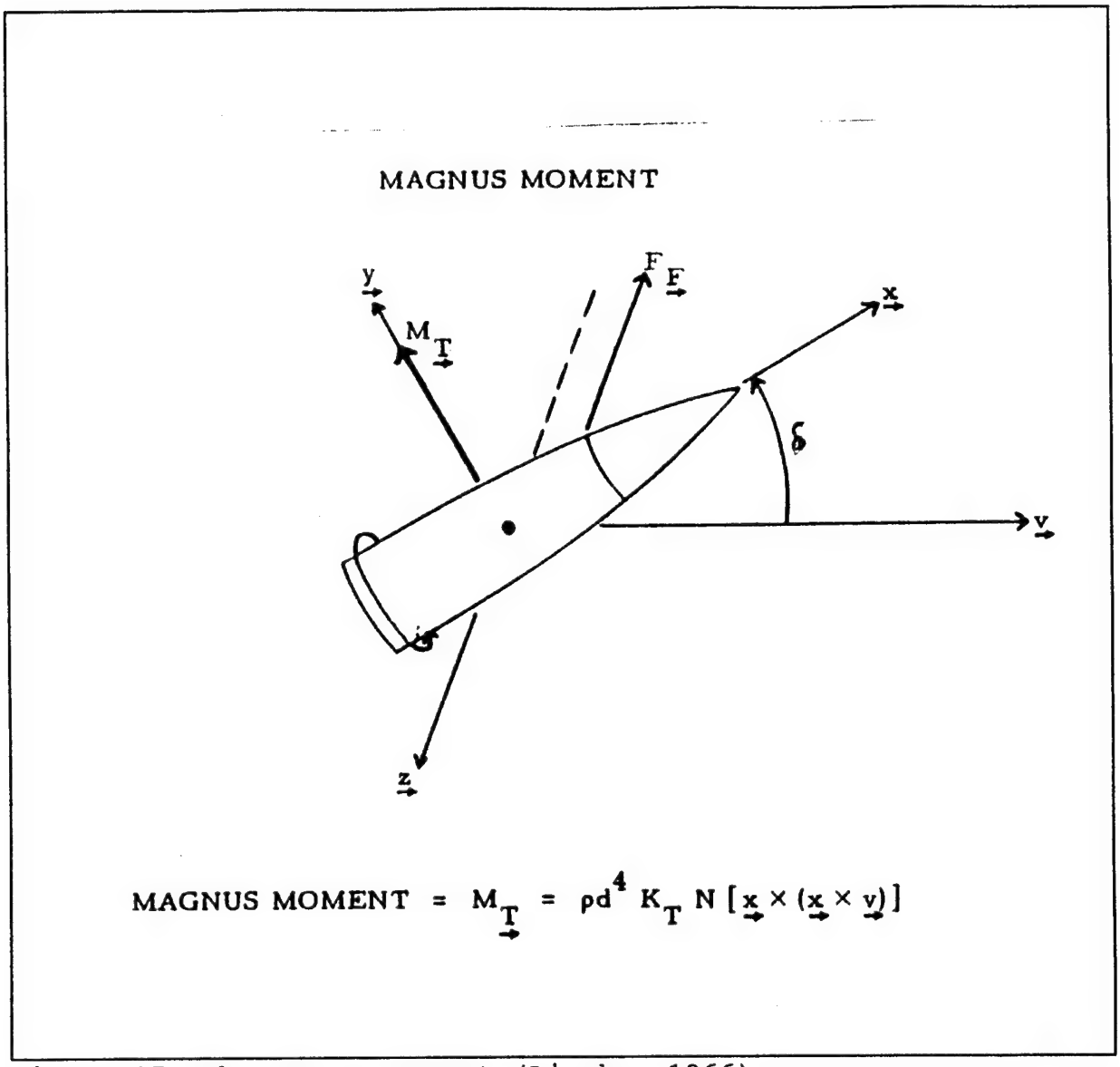

Figure 15 The Magnus moment (Lieske, 1966).

D. ESTIMATE OF REQUIRED CHANGE OF MAGNUS COEFFICIENT

The desired change in the Magnus moment coefficient can be estimated by varying the values of the coefficient and plotting the results as a function of S_2, S_3. This is done in Figures 16 and 17 below. The first Figure shows how the terms have a polarizing effect since they contain opposite signs in S_2, S_3. This is desirable since any change in the value of the coefficient may

cause an instability to result from either term. The second plot is the product of S_2, S_3 demonstrating the narrow region where stability is satisfied (the region where the product is positive). For typical values of the coefficient, a magnitude change by a factor of five may be sufficient to cause instability.

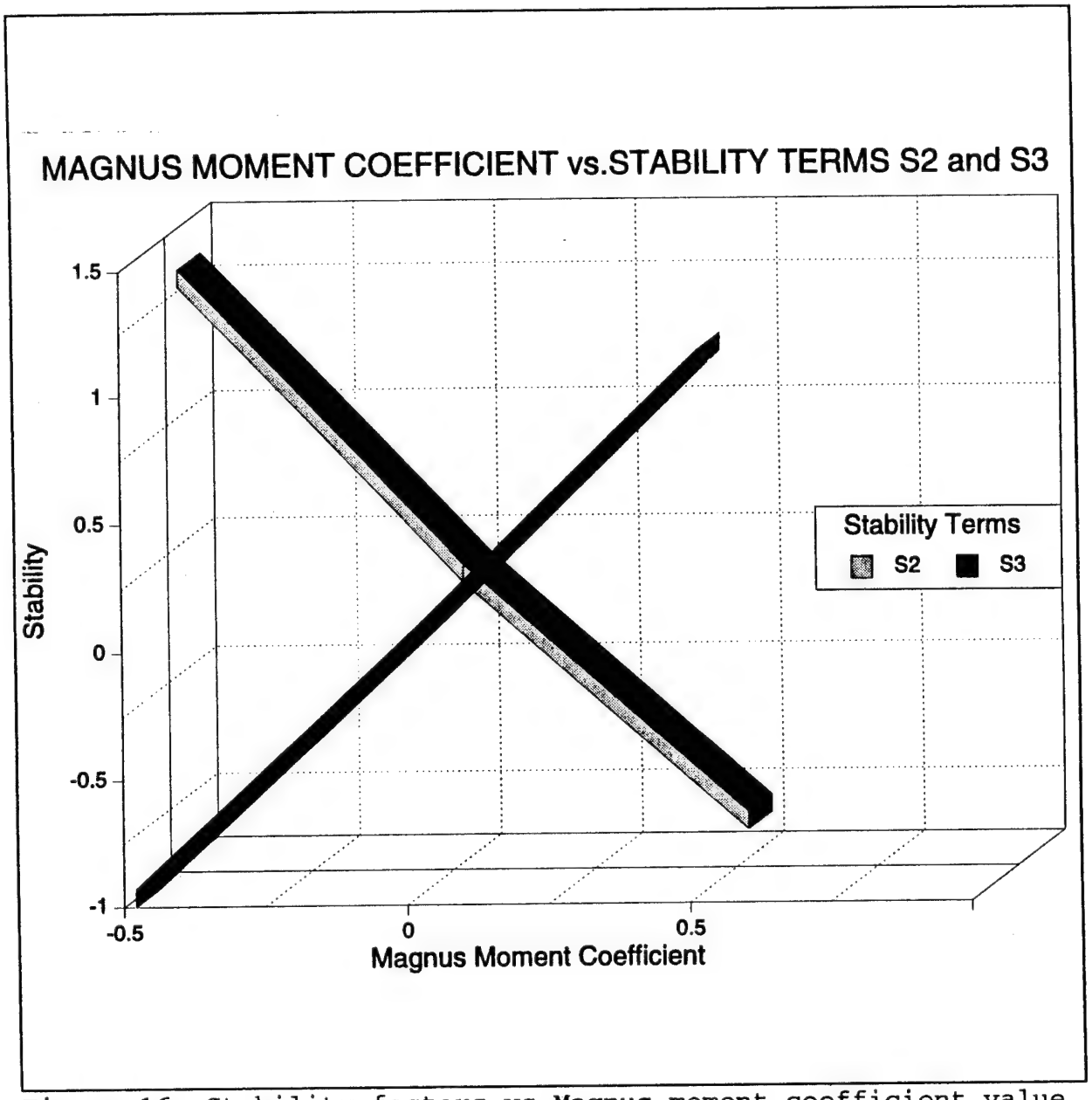

Figure 16 Stability factors vs Magnus moment coefficient value.

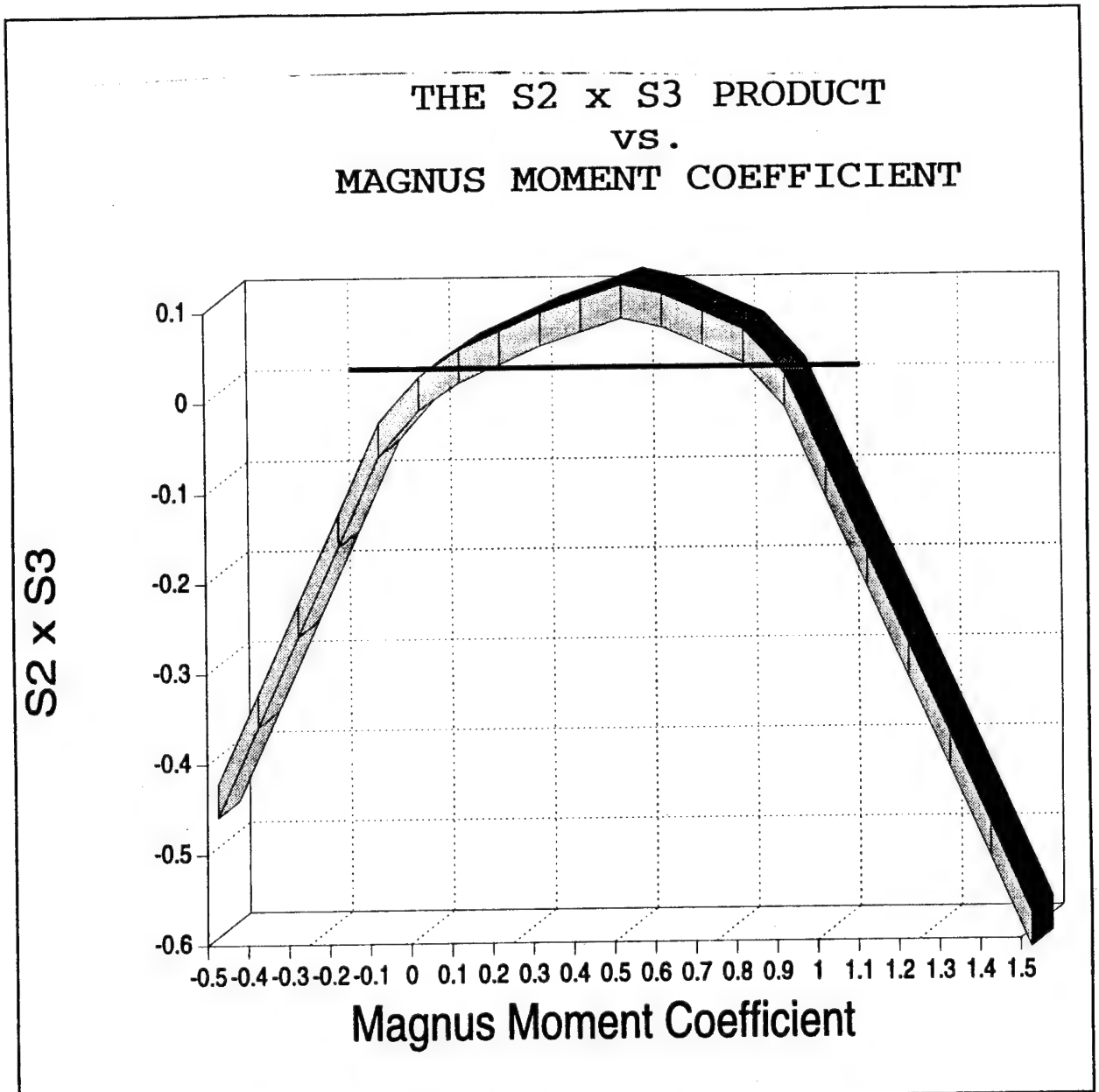

Figure 17 The stability factor product produces a region of stability for certain Magnus moment coefficients.

E. ESTIMATING YAW CHANGE VIA CHANGES IN THE MAGNUS MOMENT

The next set of calculations conducted to provide a theory for instability are based on a point mass trajectory model developed by the Ballistic Research Laboratory. The equations derived for this model provide a simplified means to calculate the yaw of repose,

$\vec{\alpha}_e$, a dimensionless expression to quantify the effect of changing yaw angle along the trajectory. The goal of the BRL was to develop a model that would incorporate the effects of yaw without the computing time of a complex rigid body simulation. The estimate was an intermediate step in achieving this goal. For this discussion, $\vec{\alpha}_e$ is the desired term for examining a magnitude effect of varying the Magnus moment (Lieske, 1966).

If the results of this calculation demonstrate a dependence of the yaw of repose on the Magnus moment, then the stability argument previously suggested is validated. The BRL found that the $\vec{\alpha}_e$ term was successful in matching empirical data when applied to equations of motion that included yaw drag and lift. They did not apply this term independently to varying conditions of the surface roughness of the projectile.

In the development of the yaw of repose estimate, the BRL used some notation that is not consistent with previous chapters. To avoid confusion and define some new terms, a list of these symbols is provided below (although Lieske et al., accounted for the Coriolis force, it has been discounted by many other studies as negligible and is ignored in this magnitude analysis as well):

B	Transverse moment of inertia
g_o	Acceleration due to gravity at ground level
$\vec{I}$	Unit vector in the direction of $\vec{v}$
K_{D_o}	Drag force coefficient
K_{D_α}	Yaw drag force coefficient

The same coordinate system previously introduced, a ground-fixed right handed Cartesian system, will be used. The body is still considered a solid of revolution and the unit vector $\vec{x}$ is along the axis of symmetry pointing forward through the nose. The magnitude of the angular velocity, N, is parallel to $\vec{x}$ and is positive for a right-handed screw motion along $\vec{x}$.

The following are the simultaneous differential equations of motion for a spin stabilized projectile. First, for the center of

mass:

$$\vec{u} = -\frac{\rho d^2}{m}(K_{D_o}+\delta^2 K_{D_\alpha})v\vec{v}+\frac{\rho d^2}{m}K_L[\vec{v}\times(\vec{x}\times\vec{v})]-\frac{\rho d^3}{m}K_s v\vec{x}+\frac{\rho d^3 K_F N}{m}(\vec{x}\times\vec{v})+\vec{g}. \qquad (3.7)$$

Recall that the total angular momentum H can be expressed by:

$$\vec{H} = AN\vec{x}+B(\vec{x}\times\dot{\vec{x}}). \qquad (3.8)$$

Therefore, the sum of the applied moments gives the vector rate of change of the angular momentum:

$$\dot{\vec{H}} = A\dot{N}\vec{x}+AN\dot{\vec{x}}+B(\vec{x}\times\ddot{\vec{x}}) = \rho d^3 K_M v(\vec{v}\times\vec{x})-\rho d^4 K_H v(\vec{x}\times\dot{\vec{x}}+\rho d^4 K_T N[\vec{x}\times(\vec{x}\times\vec{v}]-\rho d^4 K_A N v\vec{x}. \qquad (3.9)$$

Defining the yaw of repose from the rigid body system of differential equations requires these assumptions:

1) The projectile can be represented sufficiently as a body of revolution.

2) The projectile is dynamically stable.

3) The initial yaw is assumed to be small and has a negligible effect on the trajectory.

In equations 3.7 and 3.9 the magnitude $|\vec{x}\times\vec{v}|$ is present in the lift and Magnus terms. If we let $\vec{I}=\frac{\vec{v}}{v}$, then the magnitude $|\vec{x}\times\vec{I}|=\sin\delta$. Lieske, et al., then define the yaw of repose:

$$\vec{\alpha}_e \equiv \vec{I}\times(\vec{x}\times\vec{I}) = \vec{x}-\cos\delta\,\vec{I}. \qquad (3.10)$$

This vector represents the vector yaw directed from $\vec{I}$ *toward* $\vec{x}$ and is in the plane determined by $\vec{I}$, $\vec{x}$. The effect on the trajectory by $\vec{\alpha}_e$ will be small with the assumed conditions. Therefore, $\vec{\alpha}_e$ is assumed negligible yielding the following approximations:

$$\vec{x} = \cos\delta\,\vec{I}, \qquad \dot{\vec{x}} = \cos\delta\,\dot{\vec{I}}. \tag{3.11}$$

Then, dividing the total angular momentum into parallel and perpendicular components results in:

$$A\dot{N} = -\rho d^4 K_A N v, \quad AN\dot{\vec{x}} + B(\vec{x}\times\dot{\vec{x}}) = \rho d^3 K_M v(\vec{v}\times\vec{x}) - \rho d^4 K_H v(\vec{x}\times\dot{\vec{x}}) + \rho d^4 K_T N[\vec{x}\times(\dot{\vec{x}}\times\vec{v})]. \tag{3.12}$$

Then substituting x and its derivatives in 3.7 and 3.12 with equations 3.10 and 3.11 will provide a solution:

$$\vec{u} = \frac{-\rho d^2 (K_{D_o} + \delta^2 K_{D_\alpha}) v^2 \vec{I}}{m} + \frac{\rho d^2 K_L v^2 \vec{\alpha}_e}{m} - \frac{\rho d^3 K_S v \cos\delta\,\vec{I}}{m} + \frac{\rho d^3 K_F N v}{m}(\vec{\alpha}_e \times \vec{I}) + g. \tag{3.13}$$

$$AN\cos\delta\,\dot{\vec{I}} + B\cos\delta(\vec{\alpha}_e\times\dot{\vec{I}}) + B\cos^2\delta(\vec{I}\times\dot{\vec{I}}) = \rho d^3 K_M v^2(\vec{I}\times\vec{\alpha}_e) + \rho d^4 K_T N v[\cos\delta(\vec{\alpha}_e + \cos\delta\,\vec{I}) - \vec{I}] - \rho d^4 K_H v\cos\delta[(\vec{\alpha}_e + \cos\delta\,\vec{I})\times\dot{\vec{I}}].$$

Cross multiplying both sides of equations 3.13 with $\vec{I}$ and utilizing the terms, $\dot{\vec{I}}$, $\ddot{\vec{I}}$ the yaw of repose becomes:

$$\vec{\alpha}_e = \frac{[-AK_L N\cos\delta(\vec{v}\times\vec{v}) + md^2 K_T N\cos\delta[\vec{v}\times(\vec{u}-\vec{g}+\rho d^3 K_S\cos\delta\vec{v}/m)] - K_L[\vec{v} - (\vec{v}\cdot\vec{I})\vec{I}][2B\cos^2\delta(\vec{v}\cdot\vec{I}) - \rho d^4 K_H\cos^2\delta v^2]]}{[\rho d^3 K_L K_M v^4 + \rho d^5 K_F K_T N^2\cos\delta v^2 + K_L B\cos\delta[(\vec{v}\cdot\vec{I})^2 - (\vec{v}\cdot\vec{v})]]}. \tag{3.14}$$

With the v term dominating the denominator, the last term can be discarded, leaving a ratio of $\frac{g^2}{v^4}$. The middle term in the denominator after K_L can be considered approximately equal to g. With some known behavior of artillery shells this further reduces to a final form:

$$\vec{\alpha}_e = \frac{-AK_L N(\vec{v}\times\vec{u}) + md^2 K_T N[\vec{v}\times(\vec{u}-g)]}{\rho d^3 K_L K_M v^4 + \rho d^5 K_F K_T N^2 v^2}. \tag{3.15}$$

The next step is to use this equation to estimate the effects of varying the K terms. $\vec{v}\times\vec{v}$ is estimated using the ideal

trajectory, this is done by approximating $\vec{\alpha}_e^2 = \sin^2\delta$. Then, 3.15 can be written:

$$\vec{\alpha}_e = (\alpha_b - \alpha_a)(\vec{v}\times\vec{u}) - \alpha b(\vec{v}\times\vec{g}), \tag{3.16}$$

such that, $$\vec{\alpha}_e \approx (\alpha_a - 2\alpha_b)(\vec{v}_o \times \vec{g}). \tag{3.17}$$

Now the useful form desired for $\sin^2\delta$ can be written:

$$\sin^2\delta = v_o^2 g^2 (\alpha_a^2 + 4\alpha_b^2 - 4\alpha_a\alpha_b). \tag{3.18}$$

For the mathematical analysis it is necessary to define the terms α_a, α_b.

$$\alpha_a = \frac{AK_L N}{\rho d^3 K_L K_M v^4 + \rho d^5 K_F K_T N^2 v^2}, \tag{3.19}$$

$$\alpha_b = \frac{mK_T N}{\rho d K_L K_M v^4 + \rho d^3 K_F K_T N^2 v^2}.$$

It is worth noting that again, both terms contain coefficients for the Magnus moment. Using numerical values, and changing the Magnus moment coefficient from 0.3 to 1.5, the solutions for the equations 3.19 are:

$$\alpha_a \approx 9\times10^{-9}\frac{\sec^3}{ft^2}, \qquad \alpha_b \approx 4\times10^{-8}\frac{\sec^3}{ft^2}.$$

Thus the result for initial values of yaw will be:

$$\vec{\alpha}_e^2 \approx 1\times10^{-5} \approx \sin^2\delta, \qquad \delta \approx \sqrt{10}\times10^{-2}.$$

Similarly, if the Magnus moment is increased by a factor of five,

then the results are:

$$\alpha_a \approx 9\times10^{-9}, \quad \alpha_b \approx 7\times10^{-7}, \quad \vec{\alpha}_e^{\,2} \approx 1\times10^{-3}, \quad \delta \approx \sqrt{10}\times10^{-1}.$$

This is an order of magnitude change! The theoretical evidence to support instability with a five-fold magnitude increase in the Magnus moment is established. These results although not linked directly to the stability criteria support the argument that instability can be achieved with a change in the Magnus moment. Based on the stability equations, we expected instability to arise by changing the Magnus moment. Here, we have changed the Magnus moment and verified that the yaw angle will change considerably.

F. WILL THE MAGNUS EFFECT CHANGE SUFFICIENTLY WITH INCREASING THE SURFACE ROUGHNESS

A drawing of the projectile as viewed from the nose tip coming out of the page will be helpful for estimating the magnitude of the Magnus effect.

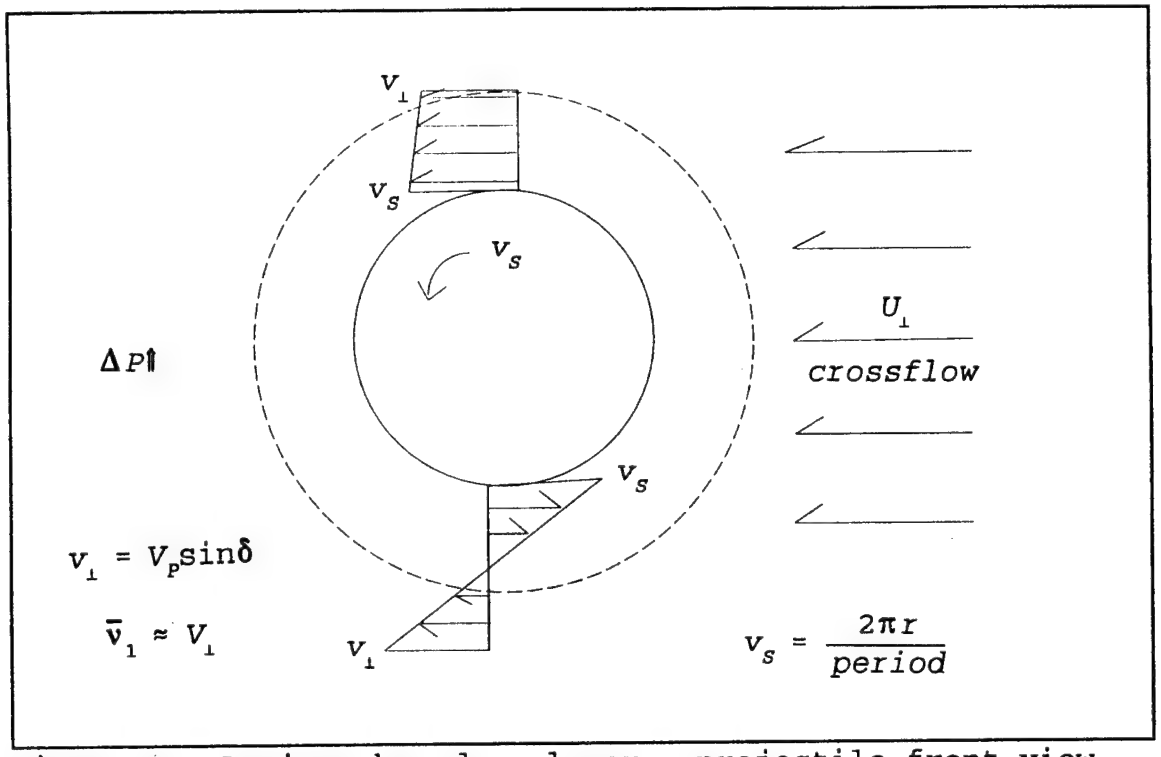

Figure 18 Laminar boundary layer - projectile front view.

The cross flow, $v_\perp$, is approximately 50 m/s for a small yaw of about five degrees. This is nearly equal to the velocity of the boundary layer close to the projectile surface (laminar flow) which is calculated to be 60 m/s. Applying the Bernoulli equation to the unroughened laminar flow projectile surface leads to the following analysis:

$$P_k + \frac{1}{2}\rho\bar{v}_1 = constant = P_o + \frac{1}{2}\rho v_\perp^2 \qquad (3.20)$$

where $\bar{v}_1 \approx v_\perp$ giving

$$P_1 + \frac{1}{2}\rho v_\perp^2 = P_o + \frac{1}{2}\rho v_\perp^2$$

and $P_1 \approx P_o$, $\bar{v}_2 \approx 0$ leading to

$$P_2 \approx P_o + \frac{1}{2}\rho v_\perp^2$$

such that

$$\Delta P_{laminar} \approx \frac{1}{2}\rho v_\perp^2$$

where

$$F_F \propto \Delta P_{laminar} \mapsto K_F \propto \frac{1}{2}\rho v_\perp^2 .$$

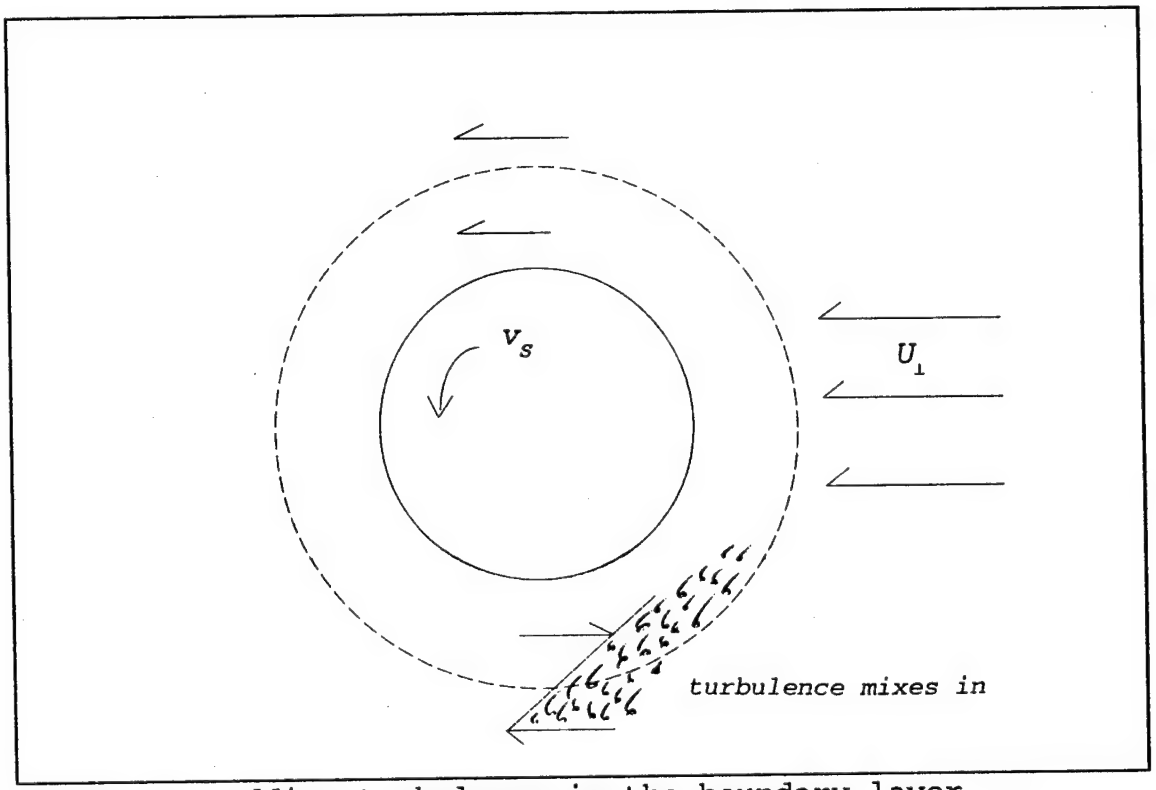

Figure 19 Adding turbulence in the boundary layer.

Adding a surface roughness, as in Figure 19, to the entire body would cause the resultant velocity vector on the lower side to decrease as fluid momentum from outside the boundary layer is drawn into the boundary layer by turbulence. The velocity along the top of the projectile will not change appreciably since the component of cross wind velocity and the velocity of the boundary layer (caused by the angular velocity of the spinning projectile) are nearly equal. The result is a small change in the Magnus force that will be estimated now.

For the projectile with a symmetric band of roughened surface, the view from the nose shows how the turbulence draws the surrounding flow into the boundary layer in the roughened region. The turbulence transports fluid momentum across the boundary layer and tends to bring the flow velocity closer to the surface. Notice the turbulence does not change the profile of the velocity along the top surface of the projectile.

The turbulent boundary layer is turbulent at a Reynolds number,

$$R_e \approx \frac{\rho v_p L}{\nu},$$

in a band around the projectile, using the full flow velocity including the longitudinal component because it is the full velocity at the boundary layer edge that determines the Reynolds number.

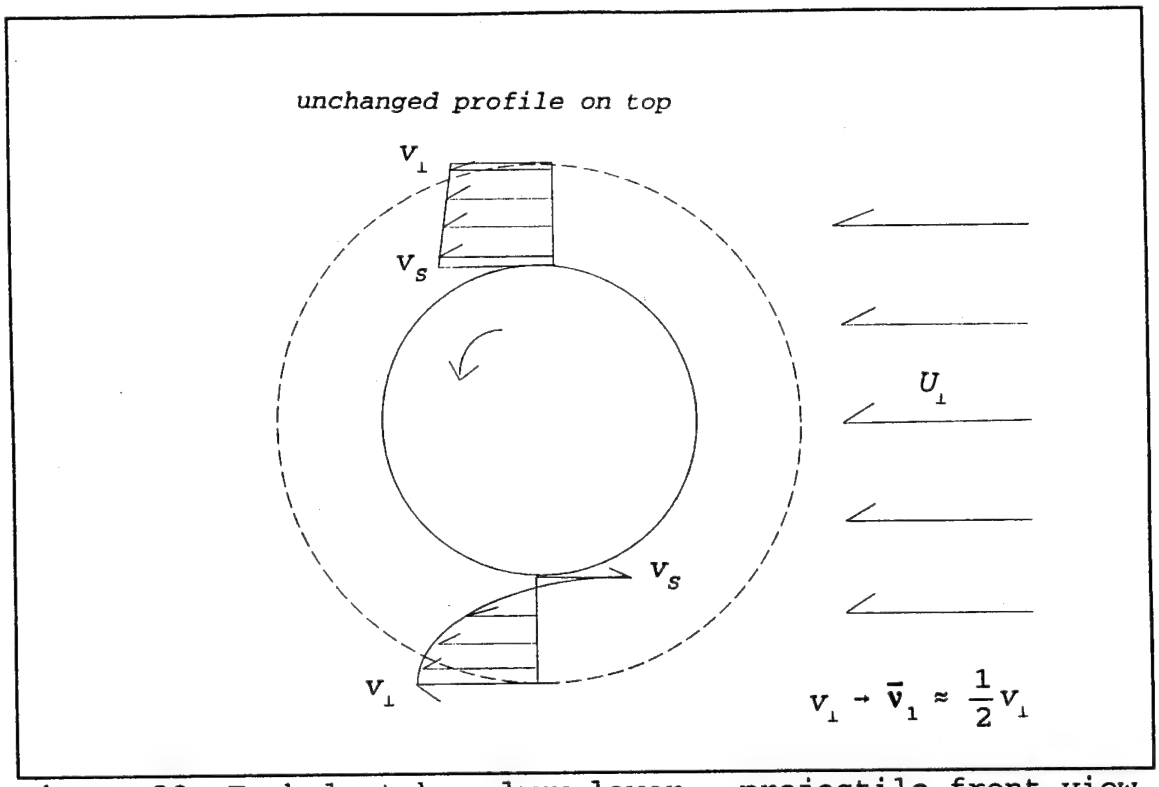

Figure 20 Turbulent boundary layer - projectile front view.

Then comparing the equations in 3.20 results in the following:

$$P_2 + \frac{1}{2}\rho\bar{v}^2 = P_o + \frac{1}{2}\rho v_\perp^2 \qquad (3.21)$$

approximating $\bar{v}_1 \approx \frac{1}{2} v_\perp$, then

$$P_2 \approx P_o + \frac{1}{2}\rho\left(v_\perp^2 - \frac{1}{4}v_\perp^2\right) = P_o + \frac{1}{2}\rho\frac{3}{4}v_\perp^2$$

such that now,

$$\Delta P_{turb} \approx \frac{3}{8}\rho v_\perp^2, \rightarrow \Delta P_{laminar} - \Delta P_{turb} = -\frac{1}{8}\rho v_\perp^2.$$

This is a change from the laminar case by a reduction of about 25% change in pressure and hence a similar change in force. But, this is only applied to the band of roughness which for a laser induced case, may only be one tenth of the length of the projectile. As a

moment arm, this would represent 20% of the moment arm length. Thus, applying a 25% decrease in Magnus force to only 20% of the surface would result in about a 5% change in the Magnus moment. This is not a significant enough effect to achieve the instability we had hoped for via the Magnus moment.

If the roughness were applied to the entire surface, the net result would only be a change in the Magnus force by a total magnitude of about 25%. This is still far short of the five-fold increase which is likely to cause an instability. There may be additional non-linear factors that contribute to the Magnus effect such as those described by the vortices that produce an additional sideforce (Platou, 1956). The analysis applying this additional component may still provide validity to the prospect of exploiting the Magnus moment as a means to achieve instability, but is not undertaken here.

The case of an asymmetric roughness does not present a uniform force that could be applied to the Magnus effect analysis. In fact, the asymmetry may only cause a wobble of the same proportions derived above. The asymmetry may also appear symmetrical to the Magnus effect if the spinning boundary layer creates a uniform turbulence at high spin rates. However, it may create a moment arm of drag which will be discussed later.

IV. AERODYNAMIC DRAG AS A MODEL

The drag will be examined as the friction factor changes by a factor of five; this value was not chosen arbitrarily, however the analysis of the Magnus effects proved that a similar change in drag would not result in an instability. As such, it is hoped that a similar magnitude change in the drag will result in an additional drag force sufficient to reduce the range of the projectile. Drag will be examined separately to determine if the effects of drag alone can prevent an incoming ballistic projectile from reaching its target.

The model for the analysis will be a cylinder to approximate a projectile. The flow through a cylinder has been, in particular, very well studied. A pipe is a cylinder with internal flow that approximates the flow behavior on the external surface as well. It has been well established that increasing surface roughness in a turbulent flow will have an effect on friction resistance. In this case, for the projectile, the effect is on the aerodynamic drag across the whole body. For the model, then, we want to increase friction resistance by a substantial factor of three to five.

The friction resistance is due to the surface effect of changing the boundary layer. By increasing surface roughness, the sublayer will break up and become increasingly turbulent.

For the 155mm ballistic projectile a roughness value, ϵ, of .046mm (White, 1979) can be divided into the length (700 mm is used as an estimate to account for the geometry) to enter Figure 21 for friction with smooth and rough walls. With a value $\frac{L}{\epsilon}$ of 15000 and using a typical Reynolds number, 10^7 for the projectile, the flow can be determined as past the transition point, but not fully turbulent. Therefore, the condition of turbulence is met and an increase in surface roughness should result in dramatic changes in the drag. In the next section, the calculations will be made that show the actual values of the Reynolds number and how the roughness must vary to provide the necessary results.

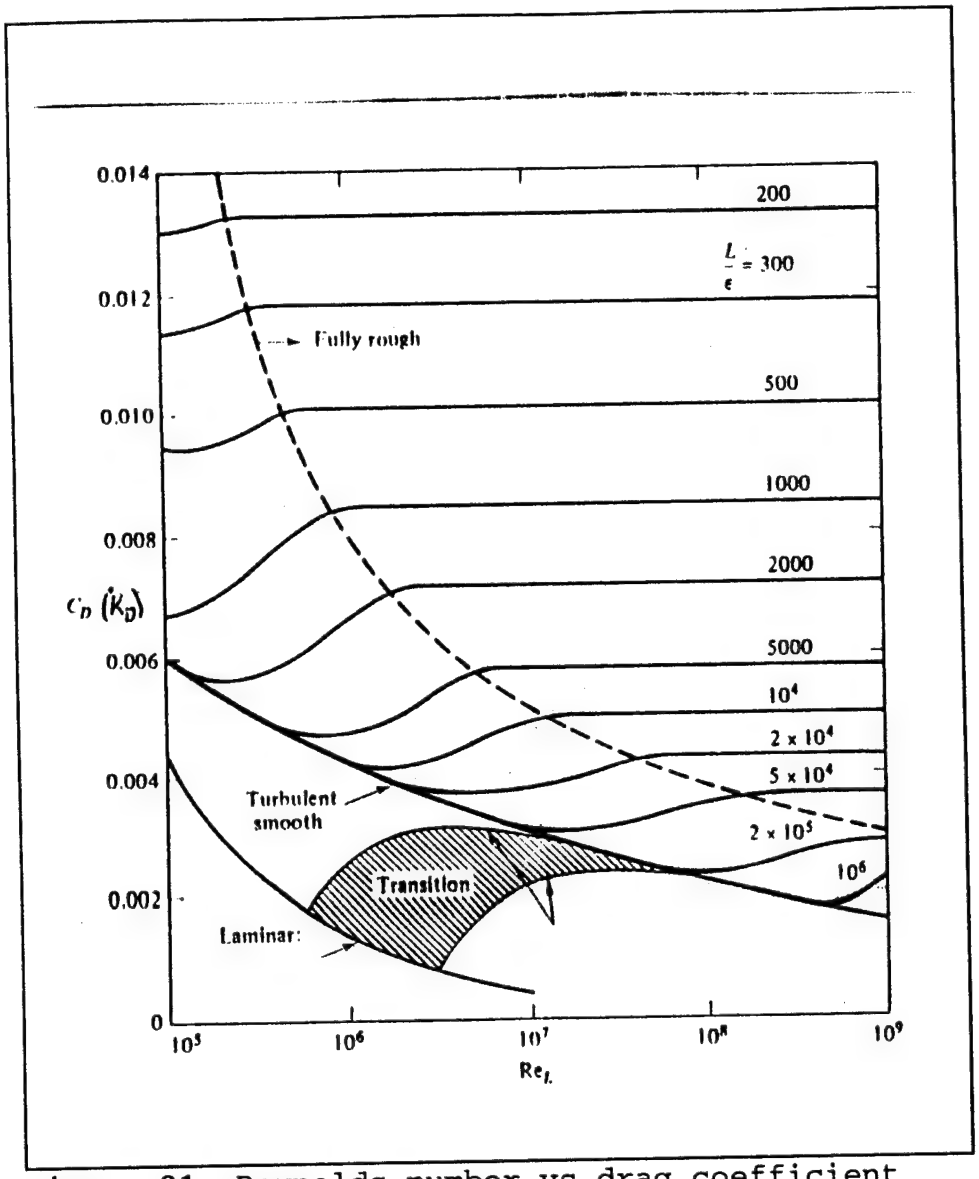

Figure 21 Reynolds number vs drag coefficient (White, 1979).

A. AERODYNAMIC DRAG ESTIMATES

The Reynolds number for our projectile must first be estimated:

$$R_{e_L} = \frac{UL}{\nu} \approx 2.6 \times 10^7 \qquad (4.1)$$

Then, entering Figure 21 with that result, and moving across

the chart with the value of $\frac{L}{\epsilon}$ = 15000 to determine the drag coefficient, gives C_D = .004. An increase of more than three can be seen on this Figure using $C_D \geq .013$ resulting in an $\frac{L}{\epsilon}$ of approximately 200. This results in a required roughness of 3.5 mm,

$$\epsilon = \frac{L}{200} = 3.5mm \tag{4.2}$$

Similarly, if the drag coefficient is used as the measure to determine a change in roughness required, it is possible to calculate the coefficient by (White, 1979):

$$K_D = \frac{.031}{R_{e_L}^{1/7}} - \frac{8700}{R_{e_L}}. \tag{4.3}$$

Using this result and multiplying it by five will again result in a change of roughness L/ϵ on the order of several hundred and a resulting roughness of several millimeters. This roughness can be visualized as dimples covering the surface of the projectile that are several millimeters deep and spaced so that no smooth surface is larger than the diameter of those dimples. The number of dimples required can be calculated using the area of the projectile and a dimple size of 5 square centimeters to be approximately 162,000. This means that the laser must pulse that many times on the incoming projectile. With a short pulse length on the order of nanoseconds, this can be done in milliseconds. A longer pulse length but no longer than microseconds will still allow sufficient roughening in under a second. With the coning and spinning motion of the projectile, a pulse rate somewhere in the middle will allow for the most dispersion of pulses over the entire body.

Similarly, a continuous pulse laser may melt the surface sufficiently in less than 1/2 second to cause the same effect. The roughness does not need to be caused by dimples. It may be equally effective to produce ridges of the same magnitude of solidified molten flow produced by the laser energy for a roughening effect.

From the criteria for vaporization equation, an approximation of the energy required can be made (Schriempf, 1974):

$$F_o\tau_p = \rho\Delta x(C_S(T_M-T_o)+L_M, \quad F_o\tau_p = \Delta x(5600\frac{J}{cm^2}), \tag{4.4}$$

where Δx is the hole size or roughness desired. Substituting in the Δx = 0.35 cm term results in the following requirement (details are located in Appendix B):

$$F_o\tau_p \approx 2 - 5\frac{KJ}{cm^2}.$$

The symmetry of the roughness does not significantly affect the net force acting on the projectile. Because the projectile is spinning and the roughness will be asymmetric over the entire body, the turbulent boundary layer will spin with the projectile as the cross wind interacts with the turbulence. In fact, an asymmetric disturbance of several thousand holes around the circumference of the spinning projectile will produce the largest increase in the drag effect since the boundary layer and hence surface friction will increase around the entire surface.

B. DRAG VS. RANGE ESTIMATE

The question remains, "how does this drag reduce the range of the projectile?" To complete this estimate, the equations of motion incorporating the drag will be used. The vertical drag will be assumed negligible compared to the axial drag for ease of estimation. This is probably a reasonable assumption anyway since the projectile will be engaged close to its terminal point and the altitude will be small compared to the range. Additionally, the yaw as the projectile reaches its target may be at its maxima providing additional lift to counter any vertical drag. This assumption also allows a starting calculation for the time of projectile flight which will be needed in the more detailed equation of motion.

$$Y = v_{Y_o} t - \frac{1}{2} g t^2. \tag{4.5}$$

Using a firing angle of 45 degrees for the projectile to achieve maximum range, the horizontal and vertical components of the velocity are equal initially ($V_{Y_o} = V_{X_o}$). The projectile is calculated to have 79.5 seconds as a time of flight.

The equation of motion used to determine range information is:

$$\ddot{x} = -\frac{d^2}{m} \rho(Y) \frac{v}{u_S(Y)} \dot{x} K_D = -\bar{G}(v) \dot{x}. \tag{4.6}$$

The functions that, in general, are dependent upon altitude will also be considered constant for the estimate made here. Applying the following steps to equation 4.6 results in a final form useful for determining the range shortfall with an increase in drag:

$$\ddot{x} = \dot{u}, \quad \dot{u} = -u\bar{G}(v), \quad \ln\frac{u(t)}{u(o)} = -\bar{G}(v)\, t,$$

$$u(t) = e^{-u(o)\,\bar{G}(v)\,t} \rightarrow x(t) = \int e^{-\bar{G}(v)\,t} dt + X_o. \tag{4.7}$$

Finally,

$$x(t) = -\frac{v_{X_o}}{\bar{G}(v)} e^{-\bar{G}(v)\,t} + X_o, \quad \textit{where} \quad X_o = \frac{v_{X_o}}{\bar{G}(v)},$$

so that

$$x(t) = \frac{v_{X_o}}{\bar{G}(v)} \left(1 - e^{-\bar{G}(v)\,t}\right).$$

Applying the final form of 4.7 to the projectile's flight in two steps will yield the desired results. First, by choosing a point 2000 meters from the CBWS the projectile's time of flight and range up to that point can be calculated. Then, using that point as the start of the engagement with a the new drag coefficient, the range of the engagement leg of flight can be compared to the range if the drag were not changed. The result, for our increase in drag is a 20% reduction in range with the engagement starting at 2000 m.

From the launch of the projectile until 2000 meters away from the target:

$$x(t) = \frac{v_{x_o}}{\frac{d^2}{m}\rho\frac{v}{u_S}\dot{x}K_D}\left(1 - e^{-\frac{d^2}{m}\rho\frac{v}{u_S}\dot{x}K_D t}\right) = 26{,}825m$$

For the remaining 2000 meters of travel new velocities in both the vertical and horizontal components must be applied in addition to an increased drag coefficient (increased from .004 to .02). The velocity will be calculated from:

$$\dot{x}(t) = v_{x_o} e^{-\bar{G}(v)\,t} \qquad (4.8)$$

where, $\bar{G}$ = .002283 for a drag factor of .004. This will give an additional projectile range during the increased drag portion ($\bar{G}$ = .008121) of its flight path of only 1619 meters. The projectile will fall short of the target by nearly 400 meters or 20 percent of the engagement distance. A twenty percent reduction in range with an easily obtainable laser requirement is an encouraging result!

C. YAW TORQUE CREATED BY A CHANGE IN ROUGHNESS

In the case where only one pulse or a series of pulses in close proximity roughen the surface of a projectile in a small area asymmetrically, there will be a torque induced that will produce an increase in yaw with the same frequency as the spinning projectile. Depending on the existing yaw angle and the cone rate, this torque may cause tricyclic motion of the projectile.

If the asymmetry is out of phase with the cone rate, it will cause a coning motion within the larger coning motion, thus a tricyclic motion as in Figure 22. This will almost always be the case. There will be points in the tricyclic motion where the yaws

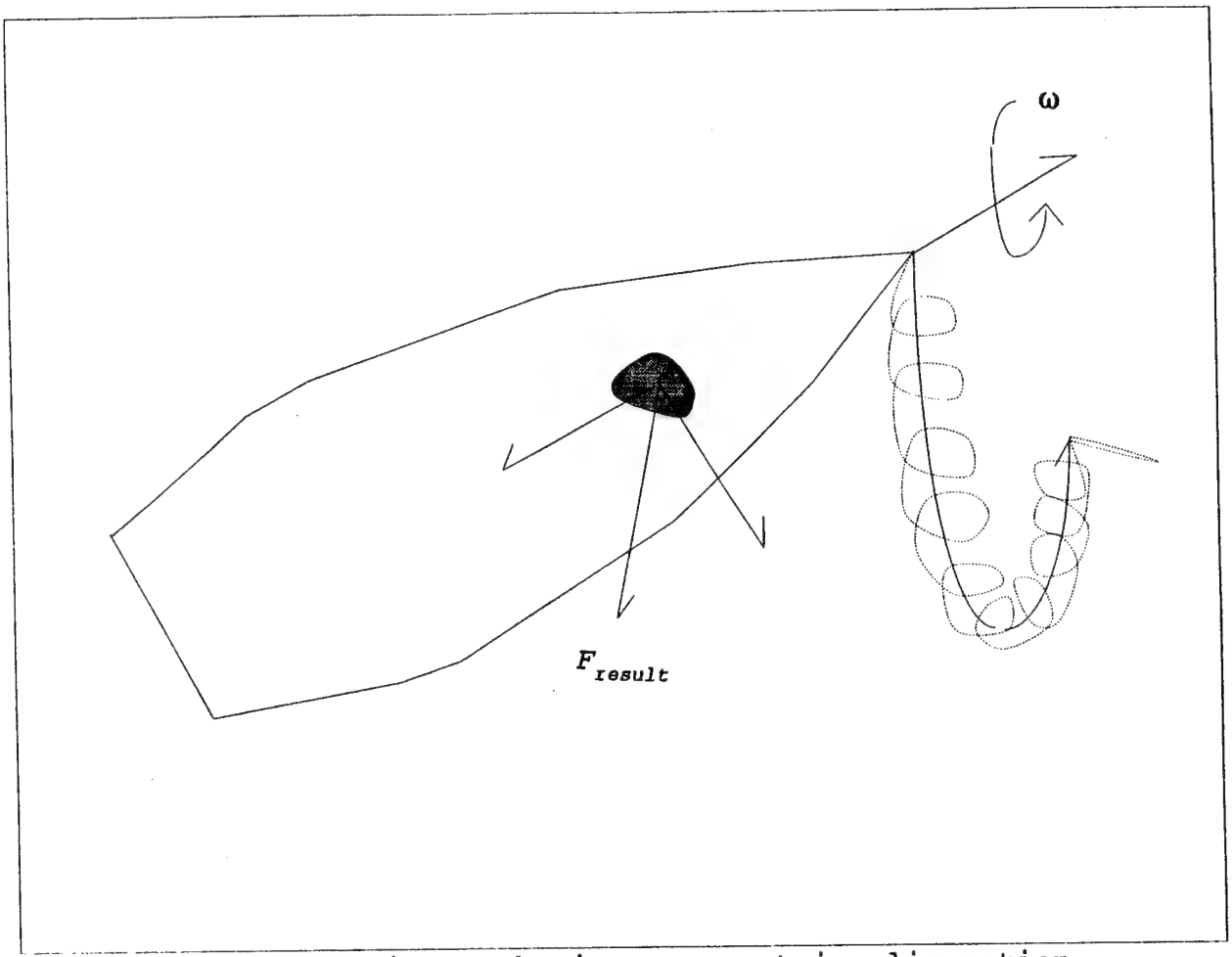

Figure 22 Asymmetric roughening causes tricyclic motion.

are complimentary and result in a larger yaw and points where the yaw motions cancel. The effects of this complex motion are difficult to describe and would vary in almost every case.

With this in mind, the projectile will be assumed to have zero cone for this calculation initially. This will enable a calculation of the contribution of the roughness independent of the other forces.

Dividing the drag force into components, the component along the axis will cause a yaw to develop. The torque created by this force is solved by the following equations:

$$\mathbf{T} = \vec{a} \times \vec{F} = |\vec{a}||\vec{F}|\sin\phi \qquad (4.9)$$

$= |\vec{a}||\vec{F}|\sin(180-\beta)$

$\geq |\vec{a}||\vec{F}|\sin(180-\gamma)$

$= |\vec{a}||\vec{F}|\sin\gamma$

$= |\vec{a}||\vec{F}|\frac{r}{a}$

$\approx r \cdot F$, *where* $r=7\,cm \approx R$.

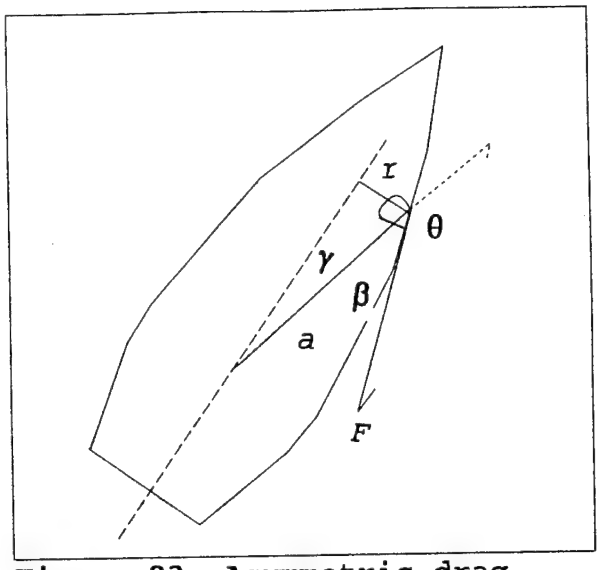

Figure 23 Asymmetric drag.

An equivalent expression is then used to solve the equation in terms of flight time remaining to the target, Δt. The change in angular momentum is related to a change of yaw angle that is chosen large enough to increase drag sufficiently to miss the target. The result is expressed below as a sequence of steps assuming there are three seconds of flight time remaining:

$$F \cdot r = \frac{\Delta L}{\Delta t} = \frac{L_S \omega \Delta \alpha}{\Delta t}, \quad \text{where } L_S = \frac{1}{2}MR^2. \qquad (4.10)$$

This results in a required force of approximately 300 Nt. But, this is not a useful number unless we can attain it with our estimated roughening that increased drag by a factor of five. For this,

$$F = \frac{1}{2}\rho u^2 C_D \cdot A, \text{ so } \Delta F = \frac{1}{2}\rho u^2 (\Delta C_D) A \approx 35\ Nt. \qquad (4.11)$$

This result is an order of magnitude less than the 300 Nt required.

V. CONCLUSIONS AND RECOMMENDATIONS

The stated goal of attaining a system that will perform the requirements set forth in the Defense Planning Guide is within the realm of physical possibilities. The use of directed energy may be a viable solution to the problem of defeating an incoming spinning ballistic projectile.

The following potential mechanisms were investigated with available theoretical models and quantitative estimates were made with the following results:

(1) Impulse transfer of momentum of 10% of the projectile momentum by laser ablation: The allowable laser energy fluences before laser absorption waves will decouple the laser from the target are orders of magnitude too small to achieve the required lateral momentum change.

(2) Impulse angular momentum change by laser impulse to increase the yaw angle significantly to induce large drag: Because of the limitation of laser pulse energy by the absorption wave threshold, it would require multiple sub-nano second multi-gigawatt pulses to achieve significant angular momentum changes.

(3) The stability of the projectile and its dependence on various aerodynamic coefficients was investigated using a well known stability model. The Magnus force and Magnus moment were identified as the most likely candidates for affecting destabilization by a five fold increase of the Magnus force. It was shown that such an increase would indeed lead to a significant change in the yaw. However, a simple analysis of the effect of surface roughening by a factor of 3-5 by laser melting or dimpling leads only to a 25% change in the Magnus force because the turbulence tends to wash out the pressure differential between the top and bottom of the projectile.

(4) The effect of increasing aerodynamic drag by laser roughening of the projectile surface was investigated. It was found that a 3-5 fold increase of surface roughness (drag) would require fluences of 2-5 Kilojoules per square centimeter and that the effect of the increased drag could lead to a 20% decrease in the projectile range over the last 2000 meters.

(5) Creation of a yaw increasing torque by a single asymmetric high roughness laser melting spot on the projectile was investigated and it was found that with a fivefold increase of roughness on a 10 square centimeter spot, the torque is too small to cause significant yaw increase and subsequent drag increase and range reduction in the time available for engagement.

The aerodynamic drag was certain to increase regardless of the Magnus effects when the surface of the projectile was roughened. The result although not dramatic emphasizes the viability of using a directed energy CBWS as a means to achieve a "kill" of an incoming enemy projectile. If the target of the projectile were a ship, then the range reduction would certainly be sufficient. For land targets, the decrease in range may pose other problems in a congested or civil warfighting environment.

The system requirements may be of a scope that is entirely different in nature. It is necessary to develop a system that is capable of tracking a projectile for ranges of several hundred meters during an engagement. This must be done with an accuracy of centimeters. The system must also be capable of determining the exact location of the projectile relative to the projectile's intended target. It would not serve its purpose to engage a ballistic projectile that was certain to overshoot its aim point if doing so would cause it to fall short and on target. These are just some of the system problems that will require addressing before a suitable CBWS could be built.

The energy requirements for the laser to induce sufficient drag are well within the bounds of current technology. In that

light, it is advisable to find an experimental means of validating these findings. There may be some interest in determining exactly how deep the laser effects will penetrate or what size melt ridges will develop on the ballistic projectile surface when atmospheric disturbances have reduced the effectiveness of the laser. A sea environment in particular, may have a deleterious effect on the directed energy against a relatively low flying target such as a terminal ballistic projectile.

Other recommendations for research include a more detailed look into the drag behavior on a projectile. The model of a flat cylinder does not take into account such things as the point where the shock wave detaches from the body. There may be other unique aerodynamic behaviors with various projectile body shapes that would require significantly more or less roughening to achieve the desired results.

Finally, one last attempt to exploit the Magnus effects is worth the effort. The nonlinear effects of the vortices shedding may be sufficient to produce the desired instability. It may be more desirable to pursue the use of a kinetic energy vehicle to cause a change in the center of mass location such that the Magnus moment causes instability. This would likely be a solution that would provide a much larger safety margin of destruction from the projectile's intended target.

APPENDIX A

Aerodynamic Forces Acting on the Projectile Preliminaries:

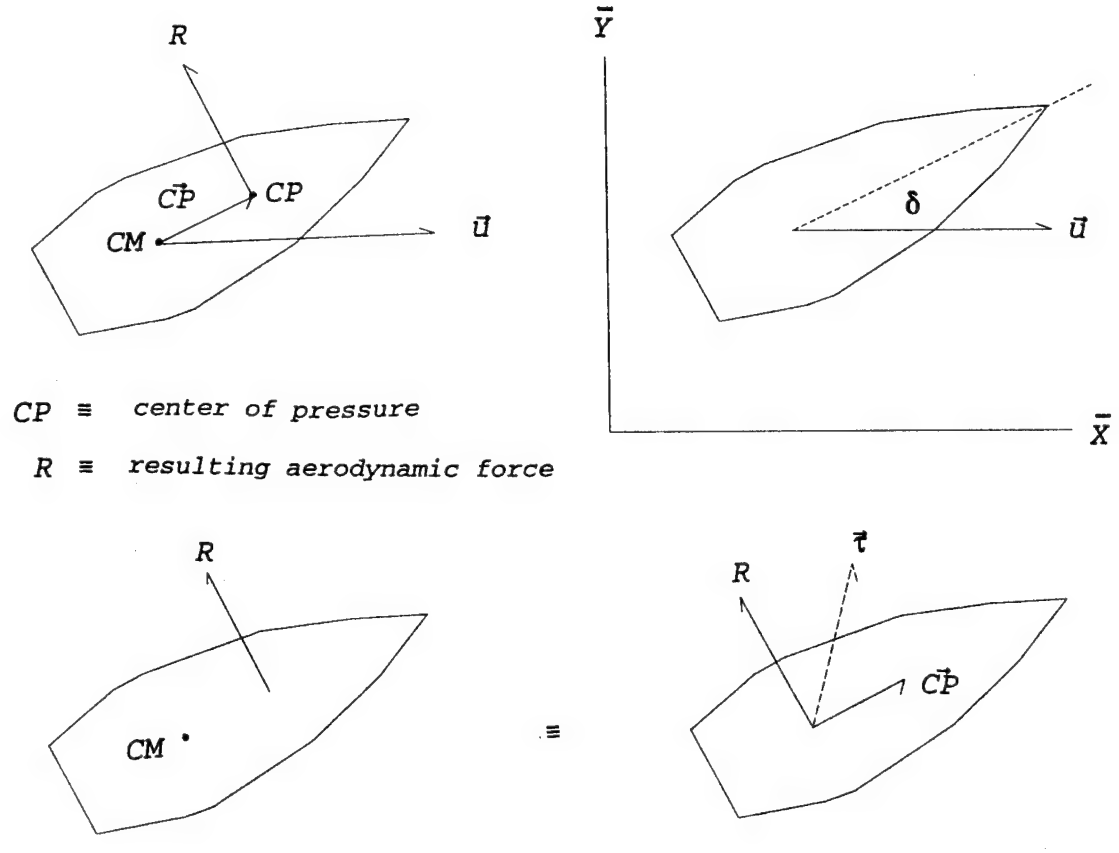

Figure 24 A single resultant force on the projectile.

For this introduction into the stability a preliminary model will be used to define some of the most basic motions and forces acting on the projectile. The projectile in the Figure above is rotationally symmetric with velocity, $\vec{u}$, with respect to the air and an angular velocity, $\vec{\omega}$, equal to zero. The terms of this Figure are defined below:

M = Overturning moment = component of $\vec{\tau}$ along the Z-axis

D = Axial Drag = component of $\vec{R}$ along the X-axis

L = Lift Force = component of $\vec{R}$ along the Y-axis

M, D, and L depend on the yaw, δ, by:

$L \equiv X\sin\delta$ *X, m are independent of* δ

$M \equiv m\sin\delta\cos\delta$

$D=\rho u^2 d^2 K_D$, $L=\rho u^2 d^2 K_L \sin\delta$, $M=\rho u^2 d^3 K_M \sin\delta\cos\delta$

$X=\rho u^2 d^2 K_L$, $m=\rho u^2 d^3 K_M$

D, m, and x are all functions of the projectile shape, diameter, velocity, sound speed and density.

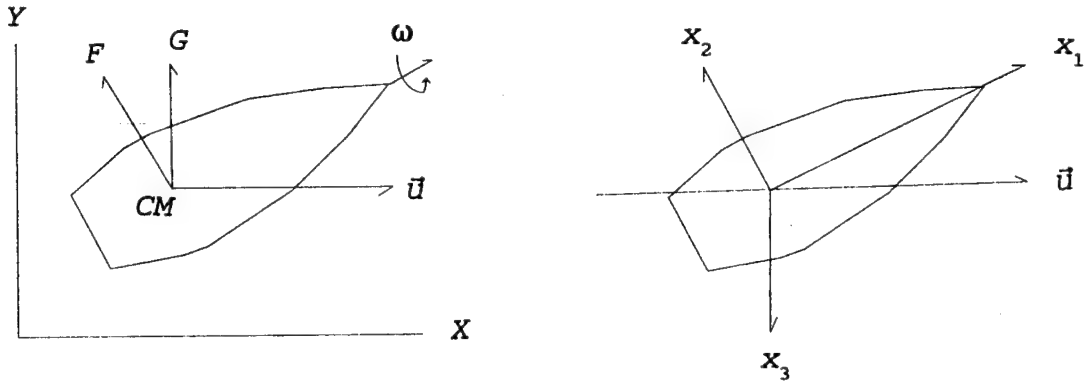

Figure 25 The forces and coordinates.

Since it is desirable to have the projectile travel with some yaw, it is necessary to impart a stabilizing spin. This will lead to a complete description of the forces acting on the projectile by reducing the aerodynamic forces to a finite number of coefficients. These have been verified experimentally within a satisfactory degree of accuracy for describing the motion of the projectile with a small yaw.

$\vec{F}(\vec{\omega},\vec{u})$ = net aerodynamic forces acting at the center of mass, *CM*.
$\vec{G}(\vec{\omega},\vec{u})$ = net torque due to aerodynamic moments.
$\hat{x}_1, \hat{x}_2, \hat{x}_3$ = unit vectors fixed to the projectile.
$\vec{F}=F_i\hat{x}_i$
$\vec{G}=G_i\hat{x}_i$
$\vec{u}=u_i\hat{x}_i$
$\vec{\omega}=\omega_i\hat{x}_i$

Then solving for F_i and G_i is done with a Taylor expansion about the unyawed position. The coefficients of the expansion are independent of $\vec{u}$ and $\vec{\omega}$ to the first order. Adding s, the angle of rotational symmetry between zero and pi, the complex numbers, $\xi=u_2+iu_3$; $\eta=\omega_2+i\omega_3$ where $u_2=\frac{1}{2}(\xi+\bar{\xi})$; $u_3=\frac{1}{2}i(\xi-\bar{\xi})$, become necessary. Linear functions of $u_2,u_3,\omega_2,\omega_3$ can be written as linear functions of $\xi,\bar{\xi},\eta,\bar{\eta}$. The Taylor expansion then becomes:

$$F_1 = a_1 + b_1\xi + b_2\eta + \bar{b}_1\xi + \bar{b}_2\bar{\eta}$$
$$\mathcal{F} \equiv F_2+iF_3 = a_2 + c_1\xi + c_2\eta + d_1\bar{\xi} + d_2\bar{\eta} \qquad \text{(A.1)}$$

The coefficients except *a* are in general complex and the special form of *F* is necessary because it must be real for all values of

ξ, η. Rotating the vectors $\hat{x}_1, \hat{x}_2, \hat{x}_3$ through the angle s about the axis of symmetry changes the axis system to $\hat{x}_1, \hat{x}_2', \hat{x}_3'$ and the following transformations take place, $\xi \to \xi\, e^{-is}$, $\eta \to \eta\, e^{-is}$, $\bar{\xi} \to \bar{\xi}\, e^{is}$ $\bar{\eta} \to \bar{\eta}\, e^{is}$, $F_1 \to F_1$, and $\mathcal{F} \to \mathcal{F}\, e^{-is}$. Because of the symmetry, such a rotation cannot change the coefficients in equations A.1. The resulting equations are:

$$F_1 = a_1 + b_1\xi\, e^{-is} + b_2\eta\, e^{-is} + \bar{b}_1\bar{\xi}e^{is} + \bar{b}_2\bar{\eta}e^{is}$$

$$\mathcal{F}\, e^{-is} = a_2 + c_1\xi\, e^{-is} + c_2\eta\, e^{-is} + d_1\bar{\xi}e^{is} + d_2\bar{\eta}e^{is} \qquad \text{(A.2)}$$

Comparing equations A.1 and A.2, the terms on the right from before and after the transformation can be set equal in F_1 *for all* ξ, η. Choose $\eta = 0$, $\xi = \bar{b}_1 \to 2b_1\,\bar{b}_1 = 2b_1\,\bar{b}_1 \cos s$, $\cos s \neq 1 \to b_1 = 0$, *similarly* $b_2 = 0$. Using the same equations to compare $\mathcal{F}$, the d terms can be examined the same way and they result in coefficient values of zero as well. Similar arguments can be made for the components of G. The result is that if a projectile is symmetric about its axis of rotation, its force and momentum system can be written to a first order approximation:

$$F_1 = a_1 \qquad \mathcal{F} = F_2 + iF_3 = C_1\xi + C_2\eta$$

$$G_1 = e_1 \qquad \mathcal{E} = G_2 + iG_3 = C_3\xi + C_4\eta \qquad \text{(A.3)}$$

where $a_1, e_1, c_1 \ldots c_4$ are functions of density, shape, velocity, angular velocity, and wind speed and are independent of the orientation of the axes $\hat{x}_1, \hat{x}_2', \hat{x}_3'$ with respect to the body. One can further show that if the projectile has a plane of mirror symmetry, then in A.3 the terms $F_1, \Re c_1, \Re c_4, \Im c_2, \Im c_3$ are even functions of ω_1 and $\mathcal{E}_1, \Re c_2, \Re c_3, \Im c_1, \Im c_4$ are odd functions.

The resulting dimensionless form of the force and moment coefficients are:

$$C_1 = -\rho d^2 u_1 K_N + i\rho d^3 \omega_1 K_F$$

$$C_2 = \rho d^4 \omega_1 K_{XF} + i\rho d^3 u_1 K_S$$

$$C_3 = -\rho d^4 \omega_1 K_T - i\rho d^3 u_1 K_M \qquad \text{(A.4)}$$

$$C_4 = -\rho d^4 u_1 K_H + i\rho d^5 \omega_1 K_{XT}$$

$$F_1 = -\rho d^2 u_1^2 K_{DA}$$

$$G_1 = -\rho d^4 u_1 K_A .$$

The K's are all even functions of ω_1 and of $\frac{u}{a}$, $d\frac{\omega}{u}$. The signs are chosen so that for a typical projectile all coefficients would be positive (for most shells, K_T is negative).

The forces and moments are then summarized as:

$\rho d^2 u_1 K_N \xi$	The Normal Force	cross force due to cross velocity.
$i\rho d^3 \omega_1 K_F \xi$	The Magnus Force	Magnus cross force due to cross velocity.
$\rho d^4 \omega_1 K_{XF} \eta$		Magnus cross force due to cross spin.
$i\rho d^3 u_1 K_S \eta$		Cross force due to cross spin.
$\rho d^4 \omega_1 K_T \xi$	The Magnus Moment	Magnus cross torque due to cross velocity.
$i\rho d^3 u_1 K_M \xi$	Over Turning Moment	cross torque due to cross velocity.
$\rho d^4 u_1 K_H$	Damping Moment or Yawing Moment	cross torque due to cross spin

$i\rho d^5 \omega_1 K_{XT}$ Magnus cross torque due to cross spin.

$\rho d^2 u_1^2 K_{DA}$ Axial Drag

$\rho d^4 u_1 \omega_1 K_A$ Spin Decelerating Moment

The force $\vec{R}$ has been resolved into forces along and perpendicular to the projectile instead of $\vec{u}$. Taking into account the yaw, δ, the normal force becomes $\rho d^2 (u\cos\delta) K_N (u\sin\delta)$, and the axial drag becomes $\rho d^2 (u\cos\delta)^2 K_{DA}$. Computing these with components along and perpendicular to the velocity vector gives:

$$\rho d^2 u^2 K_L \sin\delta = \rho d^2 u^2 K_N \sin\delta\cos^2\delta - \rho d^2 u^2 K_{DA} \sin\delta\cos^2\delta \tag{A.5}$$

$$\rho d^2 u^2 K_D = \rho d^2 u^2 K_N \sin^2\delta\cos\delta + \rho d^2 u^2 K_{DA} \cos^3\delta .$$

A comparison then gives:

$$K_L = K_N \cos^2\delta - K_{DA} \cos^2\delta \tag{A.6}$$

$$K_D = K_N \sin^2\delta\cos\delta + K_{DA} \cos^3\delta$$

which to a first order approximation ($\delta \ll 1$) is:

$$K_L \approx K_N - K_{DA} \text{ and } K_D \approx K_{DA} . \tag{A.7}$$

While the moment term, K_M, remains identical to the one previously introduced.

The general equation of motion for a symmetrical projectile has four assumptions:

1) A fixed earth three dimensional coordinate system (X, Y, Z) neglects the Coriolis force.
2) Values such as density that change with altitude are assumed constant.
3) There is no wind velocity.
4) The projectile has an angle, s, between zero and pi of rotational symmetry and a plane of mirror symmetry.

The velocity vector, angular velocity vector and projectile fixed coordinate system remain the same for the notation of this section. Equations A.3 represent the Aerodynamic force and the Aerodynamic torque, respectively. A unit vector parallel to the vertical axis in the earth fixed system is defined to be $Y_1 \rightarrow \Upsilon = Y_2 + iY_3$ and the acceleration due to gravity transforms $-gY_1 \rightarrow -g\Upsilon$. The remaining terms to introduce are: the moment of inertia about the axis of the projectile, A; the moment of inertia about any axis perpendicular to the projectile axis through the center of mass, B; and the mass of the projectile, m.

The general equation of motion is:

$$\frac{d}{dt}(m,\vec{u}) = \vec{F} - mg\hat{y}. \tag{A.8}$$

The angular momentum equation in the projectile coordinate system is given by:

$$\vec{\mathfrak{L}} = A\omega_1\hat{x}_1 + B\omega 2\hat{x}_2 + B\omega_3\hat{x}_3 = (A-B)\,\omega_1\hat{x}_1 + B\vec{\omega}$$

and $\dfrac{d\vec{\mathfrak{L}}}{dt} = \vec{G}$, $\dfrac{d}{dt}\{(A-B)\,\omega_1\hat{x}_1 + B\vec{\omega}\} = \vec{G}$. (A.9)

The time derivative of vector $\vec{P}$ is expressed in the projectile system where P transforms, $\vec{P} \rightarrow \{P_1; \wp = P_2 + iP_3\}$. Using index notation, $\vec{P} = P_i\hat{x}_i$ and $\dot{\vec{P}} = \dot{P}_j\hat{x}_j + P_j\dot{\hat{x}}$. The vectors $\hat{x}_j$ are fixed in the projectile.

$$\dot{\vec{P}} = \dot{P}_j\hat{x}_j + P_j\vec{\omega}\times\hat{x}_j$$

$$\hat{x}_j = \vec{\omega} \times \hat{x}_j$$

(A.10)

$$\vec{P} \cdot \hat{x}_k = \dot{P}_j \delta_{jk} + P_j (\vec{\omega} \times \hat{x}_j) \cdot \hat{x}_k = \dot{P}_k - P_j (\vec{\omega} \cdot (\hat{x}_k \times \hat{x}_j)$$

In components, the first one becomes:

$$\vec{P} \cdot \hat{x}_1 = \dot{P}_1 + [(P_2 + iP_3)(\omega_2 - \omega_3) - (P_2 - iP_3)(\omega_2 + i\omega_3)] \frac{i}{2} = \dot{P}_1 + (\rho\bar{\eta} - \bar{\rho}\eta) \frac{i}{2}.$$

(A.11)

The second and third added together with the third multiplied by i becomes:

$$\vec{P} \cdot \hat{x}_2 + i\vec{P} \cdot \hat{x}_3 = \dot{P}_2 + i\dot{P}_3 - iP_1(\omega_2 + i\omega_3) + i\omega_1(P_2 + iP_3) = \dot{\rho} - iP_1\eta + i\omega_1\rho \quad \text{(A.12)}$$

So, the equation of motion in projectile based coordinates are:

$$m[\dot{u}_1 - (\xi\bar{\eta} - \bar{\xi}\eta) \frac{i}{2}] = F_1 - mg_1$$

$$m[\dot{\xi} - iu_1\eta + i\omega_1\xi] = \mathcal{F} - mg\Upsilon = C_1\xi + C_2\eta - mg\Upsilon. \quad \text{(A.13)}$$

And, the equations for the angular momentum are:

$$\frac{d}{dt}(A-B)\omega_1\hat{x}_1 + B\vec{\omega} = \vec{G}. \quad \text{(A.14)}$$

The above lema on the time derivative gives:

$$\frac{d}{dt}[\omega_1\hat{x}_1] = \begin{cases} \dot{\omega}_1 + (0 \cdot \bar{\eta} - 0 \cdot \eta) \frac{i}{2} = \dot{\omega}_1 \\ 0 \quad -i\omega_1\eta \quad + \quad 0 \quad = -i\omega_1\eta \end{cases} \qquad \text{and}$$

$$\frac{d}{dt}[\vec{\omega}] = \begin{cases} \dot{\omega}_1 + (\eta\cdot\bar{\dot{\eta}} - \dot{\eta}\cdot\eta)\frac{i}{2} = \dot{\omega}_1 \\ \dot{\eta} \quad -i\omega_1\eta \quad +i\omega\eta \quad = \dot{\eta}. \end{cases}$$

With this we have the two equations:

$$(A-B)\dot{\omega}_1 + B\dot{\omega}_1 = G_1$$

$$(A-B)(-i\omega_1\eta) + B\cdot\dot{\eta} = \mathscr{E} = C_3\xi + C_4\eta \qquad \text{(A.15)}$$

The differential equation for a change in the force of gravity in the projectile frame is given by assuming $\vec{Y}$ = *constant*, $\dot{\vec{Y}} = 0$ in the lab frame and applying the lema:

$$\frac{d}{dt}[\hat{Y}] = \begin{cases} \dot{Y}_1 + (\Upsilon\bar{\eta} - \bar{\Upsilon}\eta)\frac{i}{2} \\ \dot{\Upsilon} - iY_1\eta + i\omega\Upsilon. \end{cases} \qquad \text{(A.16)}$$

There is however an altitude dependence on the speed of sound and the density. The altitude change of the projectile must be tracked in order to insert the correct $\rho(Y)$, $a(Y)$ values. If $\vec{u}$ has a component $\vec{u}\cdot\hat{Y}$ in altitude direction then its altitude change is given by:

$$\dot{Y} = \vec{u}\cdot\hat{Y} = u_1Y_1 + u_2Y_2 + u_3Y_3 = u_1Y_1 + \frac{1}{2}(\xi\bar{\Upsilon} + \bar{\xi}\Upsilon). \qquad \text{(A.17)}$$

The normal equation of motion is then derived. Again, several simplifications are introduced to get an approximate trajectory before making corrections:

1) The projectile axis is tangent to the trajectory.
2) The only forces acting on the projectile are drag and gravity.
3) The variables affected by altitude are considered constant.
4) There is no wind.

The projectile will remain in the vertical plane of the initial velocity vector as indicated by Figure 26.

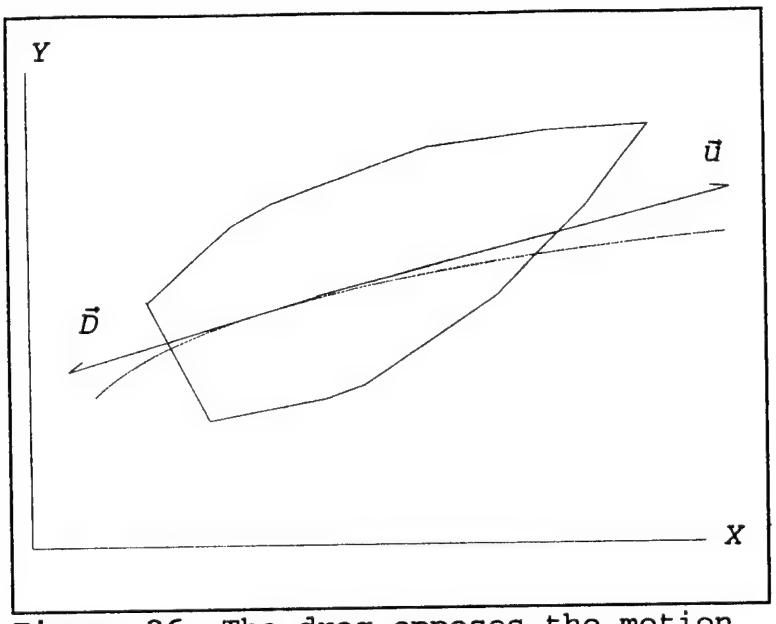

Figure 26 The drag opposes the motion.

$$D = \rho d^2 u^2 K_D, \quad u^2 = \dot{X}^2 + \dot{Y}^2, \quad \vec{D} = -\rho d^2 u^2 K_D \frac{\vec{u}}{u}, \quad \vec{F}_g = -\hat{Y} mg$$

The equations of motion are then:

$$m\ddot{u} = -\rho D^2 u K_D \dot{u} - mg\hat{Y} \tag{A.18}$$

with components:

$$m\ddot{X} = -\rho d^2 u K_D \dot{X}, \quad m\ddot{Y} = -\rho d^2 u K_D \dot{Y} - mg \tag{A.19}$$

where $K_D = K_D(\frac{u}{a})$, $u^2 = \dot{X}^2 + \dot{Y}^2$, $\rho = \rho(Y)$, $a = a(Y)$. Most exterior ballistics involves the precise integration of equations A.19.

The standard form of a normal solution is given by:

$\dot{X} = u\cos\theta$, $\dot{Y} = u\sin\theta$

and $\ddot{X} = \dot{u}\cos\theta - u\sin\theta\,\dot{\theta}$, $\ddot{Y} = \dot{u}\sin\theta + u\cos\theta\,\dot{\theta}$, so that

$$m\dot{u}\cos\theta - mu\sin\theta\,\dot{\theta} = -\rho d^2 K_D u^2 \cos\theta \tag{A.20}$$

and $m\dot{u}\sin\theta + mu\cos\theta\,\dot{\theta} = -\rho d^2 K_D u^2 \sin\theta - mg$.

Multiplying the third and fourth equations above by cos and sin respectively, then adding the result gives:

$$m\dot{u} = -\rho d^2 K_D u^2 - mg\sin\theta. \qquad \text{(A.21)}$$

Similarly, multiplying by sin and cos respectively then subtracting gives:

$$\dot{\theta} = -\frac{g}{u}\cos\theta \qquad \text{(A.22)}$$

To the above equations A.21 and A.22 the following terms are added: $\rho=\rho(Y)$, $a=a(Y)$, $K_D=K_D(\frac{u}{a})$.

Next, the angular motion of the projectile will be discussed starting with the simplification of the equation of motion, equations A.13 and the following:

$$\begin{aligned} A\dot{\omega}_1 &= G_1 \\ B\dot{\eta} + (B-A)i\omega_1\eta &= \mathscr{E} \\ \dot{Y}_1 &= (\Upsilon\bar{\eta} - \bar{\Upsilon}\eta)\frac{i}{2} \\ \Upsilon &= iY_1\eta - i\omega_1\Upsilon \\ \dot{Y} &= u_1 Y_1 + \frac{1}{2}(\xi\bar{\Upsilon} + \bar{\xi}\Upsilon) \end{aligned} \qquad \text{(A.23)}$$

where $\mathscr{F} = C_1\xi + C_2\eta$, $\mathscr{E} = C_3\xi + C_4\eta$, and the values $C_1 \ldots C_4$, F_1, G_1 in terms of the aerodynamic coefficients are given.

Changing the notation somewhat to include a density factor, $\rho\frac{d^3}{m}$, is necessary. The density factor is applied to the aerodynamic coefficient to result in J terms, $J_o = \rho\frac{d^3}{m}K_\rho$. Further, we will define the spin per caliber travel as: $\nu = \omega_1\frac{d}{u_1}$. The coefficients then become:

$$\begin{aligned} C_1 &= (-J_N + i\nu J_F)m\frac{u_1}{d} \\ C_2 &= (\nu J_{KF} + iJ_S)mu_1 \\ C_3 &= (-\nu J_T - iJ_M)mu_1 \\ C_4 &= (-J_H + i\nu J_{XT})mu_1 d \\ G_1 &= -J_A \nu U_1^2 m. \end{aligned} \qquad \text{(A.24)}$$

Then use approximation by means of the normal equation of motion. Let the center of mass motion be governed by the normal equation of motion:

$$\dot{u} = -\rho d^2 u^2 \frac{K_D}{m} - g\sin\theta = -u^2 \frac{J_D}{d} - g\sin\theta$$

$$\dot{\theta} = -g\cos\frac{\theta}{u} \tag{A.25}$$

$$\dot{X} = u\cos\theta, \qquad \dot{Y} = u\sin\theta.$$

The solution is assumed to be known and satisfies

$$\dot{U} = -J_D \frac{U^2}{d} - g\sin\theta. \tag{A.26}$$

Next, we will conduct a change of independent variables starting in the yaw equations. First replace:

$$P = \int_0^t \frac{u_1}{d}\, dt = \int_0^t (\frac{U}{d})\, dt. \tag{A.27}$$

This is then the arc length along the trajectory in calibers. The equations determining the yaw motion will become essentially independent of the size of projectile. A large projectile has the same period of yaw measured in calibers of travel as a small model.

$$(\dot{Q}) = \frac{dQ}{dP}\frac{u_1}{d} = \frac{dQ}{dP}\frac{U}{d} \equiv Q'\frac{U}{d} \tag{A.28}$$

The trajectory normal equations are then:

$$U' = -J_D U - gd\sin\frac{\theta}{U}, \quad \theta' = -gd\cos\frac{\theta}{U^2}. \tag{A.29}$$

The equation for the derivative of the angular velocity becomes:

$$A\dot{\omega}_1 = G_1 \rightarrow \omega_1' = \frac{dG_1}{AU} = -d\nu m \frac{J_A}{A}\frac{U^2}{U} \text{ with } \omega_1 = \frac{U}{d}\nu, \ \omega' = \nu'\frac{U}{d} + \frac{\nu}{d}U'.$$

Therefore, $\nu' \frac{U}{d} + \frac{\nu}{d} U' = -d\nu m J_A \frac{U}{A}$, $\nu' = -\frac{\nu}{U} U' - d^2 \nu m \frac{J_A}{A}$ resulting in:

$$\nu' = -\frac{J_A}{A} m d^2 + \nu J_D + \nu g d U^{-2} \sin\theta . \qquad \text{(A.30)}$$

To change dependent variables the variables, ξ, η, Y_1, Υ are changed as follows:

$$\lambda = \frac{\xi}{U} e^{i\int_0^P \nu dp} \qquad \mu = \eta \frac{d}{U} e^{i\int_0^P \nu dp}$$

$$\gamma = g\Upsilon e^{i\int_0^P \nu dp} \qquad g_1 = gY_1 .$$

$\frac{\xi}{U}$ is the vector yaw which has the magnitude of the sine of the angle of yaw. The factor

$$e[i\int_0^P \nu dp] = e[i\int_0^t \omega_1 dt]$$

changes the coordinate system from $\hat{x}_1$, $\hat{x}_2$, $\hat{x}_3$ which rotates with the projectile to one that does not rotate about the $\hat{x}_1$-axis.

The quantity, λ, is the complex yaw measured from the axis of the projectile to the trajectory on a coordinate system with one axis along the projectile axis and which is not spinning about the axis. Similarly, μ, γ, g, have interpretations. The coordinate system thus described is determined when we fix the direction of $\hat{x}_2$.

The aerodynamic force perpendicular to the projectile axis is,

$$\mathcal{F} = (-J_N + i\nu J_F) mU \frac{\xi}{d} + (\nu J_{XF} + iJ_S) mU\eta$$

and in the non-rotating system the lateral force is this quantity multiplied by

$e^{i\int_0^P \nu\, dp} \rightarrow \mathcal{F}^{(1)}$. This equation then becomes

$$\mathcal{F}^{(1)} = (-J_N + i\nu J_F)\, mU^2 \frac{\lambda}{d} + (\nu J_{XF} + iJ_S)\, mU^2 \frac{\mu}{d}. \qquad \text{(A.31)}$$

The component of drag in the plane perpendicular to the projectile is due to an aerodynamic force acting on the projectile with the complex number representation, $\mathcal{F}^{(1)}$, together with that component of the axial drag which is in the $\mathcal{R}_2''$-$\mathcal{R}_3''$ plane. This component is $\lambda J_D U^2 \frac{m}{d}$. The aerodynamic force perpendicular to the projectile has the complex number representation described by: $[(J_D - J_N + i\nu J_F)\lambda + (\nu J_{XF} + iJ_S\mu)]\, m\frac{u^2}{d}$. The real axis is perpendicular to the trajectory pointing downward and the imaginary axis is horizontal pointing to the left. The quantities λ and μ are the cross velocities divided by the axial velocity U and the cross angular velocity multiplied by d/U.

The final form of the equation is then obtained. For the sake of abbreviation, the term $\int_0^P \nu\, dp \equiv \varphi$. Making the same transformations for ξ, η, Υ:

$$\xi = \xi' \frac{U}{d} = (\lambda U e^{-i\varphi})' \frac{U}{d} = [\lambda' U + \lambda(-J_D - gdU^{-2}\sin\theta)\, U - i\gamma\lambda U]\, e^{-i\varphi} \frac{U}{d}$$

$$= [\lambda' - i\nu\lambda - \lambda(J_D + gdU^{-2}\sin\theta)]\, \frac{U^2}{d} e^{-i\varphi}. \qquad \text{(A.32)}$$

Similarly,

$$\eta = [\mu' - i\gamma\mu - \mu(J_D + gdU^{-2}\sin\theta)]\, \frac{U^2}{d^2} e^{-i\varphi} \qquad \text{(A.33)}$$

and $g\Upsilon = (\gamma' - i\nu\gamma)\frac{U}{d} e^{-i\varphi}$. $\qquad$ (A.34)

These are now inserted into equations A.23 leading to the following

equations:

$$m[\lambda' - \lambda(J_D + gdU^{-2}\sin\theta) - i\mu] = (C_1\xi + C_2\eta - mg\Upsilon)\frac{d}{U^2}e^{i\varphi} = C_1\lambda\frac{d}{U} + C_2\mu\frac{1}{U} - m\gamma\frac{d}{U^2}$$

$$B[\mu' - \mu(J_D + gdU^{-2}\sin\theta)] - iA\nu\mu = C_3\lambda\frac{d^2}{U} + C_4\mu\frac{d}{U} \qquad \text{(A.35)}$$

$$\gamma' = ig\mu, \qquad g_1' = (\gamma\bar{\mu} - \bar{\gamma}\mu)\frac{i}{2}.$$

Substituting in the constants $C_1 \ldots C_4$, G_1, $\frac{B}{md^2} \equiv k^2$ (the transverse radius of gyration in calibers) gives:

$$\lambda' = (J_D - J_N + i\nu J_F + gdU^{-2}\sin\theta)\lambda + (\nu J_{XF} + iJ_S + i)\mu - \gamma dU^{-2}$$

$$\mu' = (-\nu J_T - iJ_M)\lambda k^{-2} + (J_D - k^{-2}J_H + i\nu k^{-2}J_{XT} + gdU^{-2}\sin\theta + iA\frac{\nu}{B})\mu$$

$$\gamma' = ig\mu, \qquad g_1' = (\gamma\bar{\mu} - \bar{\gamma}\mu)\frac{i}{2}. \qquad \text{(A.36)}$$

Finally, the solution of the equation of motion will be completed by using some approximations which will simplify equations A.36:

1) Each J-term contains a density factor that is very small in magnitude, on the order of 10^{-4}.
2) A/B will be approximately 1/10.
3) As with the density factor, $\frac{gd}{U^2} < 10^{-3}$.
4) Derivatives of the J-terms are negligible.

The equations A.36 will be abbreviated as follows:

$$\lambda' = a_1\lambda + a_2\mu + b$$
$$\mu' = a_3\lambda + a_4\mu \qquad \text{(A.37)}$$

with the constants equal to:

$$a_1 = J_D - J_N + i\nu J_E$$

$$a_2 \approx \nu J_{XF} + i$$
$$a_3 \approx (-\nu J_T - i J_M) k^{-2}$$
$$a_4 \approx (J_D - k^{-2} J_H + g d U^{-2} \sin\theta + i \frac{A}{B} \nu)$$
$$b = (g\lambda \sin\theta - \gamma) d U^{-2}.$$

Next, we will eliminate μ from equations A.37 by substituting the first into the second equation:

$$\lambda'' + \lambda' (-a_1 - a_4 - \frac{a_2'}{a_2}) + \lambda (a_1 a_4 - a_2 a_3 + a_1 \frac{a_2'}{a_2} - a_1') + b(\frac{a_2'}{a_2} + a_4 - \frac{b'}{b}) = 0.$$

To deal with the derivative term a_2', recall equation A.30. The terms $\frac{a_2'}{a_2}$, a_1' are of the order of J^2, whereas the other terms in the coefficients are of the order of J. So, they can be neglected. The result is:

$$\lambda'' + \lambda' (-a_1 - a_4) + \lambda (a_1 a_4 - a_2 a_3) + b(a_4 - \frac{b'}{b}) = 0. \qquad \text{(A.38)}$$

The solution of the homogeneous part of A.38 is done with a change of variable to eliminate the first derivative term (the particular solution will be addressed later):

$$\lambda \to q e^{\frac{1}{2}\int_0^P (a_1 + a_4)\, dp}. \qquad \text{(A.39)}$$

From this equation, the two derivatives $\lambda' = [q' + \frac{1}{2}(a_1 + a_4) q] e^{\alpha}$ and $\lambda'' = [q'' + (a_1 + a_4) q' + \frac{1}{4}(a_1 + a_4)^2 q + \frac{1}{2}(a_1 + a_4)' q] e^{\alpha}$ are found. Substituting these into A.38 gives:

$$q'' - r^2 q = 0 \qquad \text{(A.40)}$$

where r^2
$= \frac{1}{4}[(a_1 + a_4)^2 - 4(a_1 a_4 - a_2 a_3) - 2(a_1 + a_4)'] = \frac{1}{4}[(a_1 - a_4)^2 + 4 a_2 a_3 - 2(a_1 + a_4)']$.

To find the approximate solution of equation A.40, let $Z \equiv (\ln q)' = \frac{1}{q} q'$; $Z' = -\frac{1}{q^2} q'^2 + \frac{q''}{q} = -Z^2 + r^2$. Then, $Z' + Z^2 - r^2 = 0$. If r were constant then the equation would have a solution $Z = \pm r$. r^2 is not really constant because of the ν in the $a_1 \ldots a_4$ terms, but r is nearly constant which allows a trial solution of $Z = r + \epsilon, \epsilon \ll r$. It follows $\epsilon' + 2r\epsilon + \epsilon^2 + r' = 0$. Let $\epsilon = -\frac{r'}{2r}$ then neglecting ϵ', ϵ^2 quantities satisfies the equation approximately. The error is of the order $(\epsilon' + \epsilon^2)/r^2$. The solution is then:

$$Z \approx r - \frac{r'}{2r}$$

and hence,

$$q = e^{\int_0^P (r - \frac{r'}{2r}) \, dp} . \qquad \text{(A.41)}$$

Using the other sign in $Z = \pm r$,

$$q = e^{\int_0^P [-\frac{r'}{2r}) \pm r] \, dp} . \qquad \text{(A.42)}$$

Solving for λ, we also expect two solutions:

$$\lambda = e^{\int_0^P [a_1 + a_4 - \frac{r'}{r}) / 2 \pm r] \, dp} . \qquad \text{(A.43)}$$

Now, to express the coefficients in A.43 in terms of aerodynamic coefficients, the coefficients $a_1 + a_4$ from A.37 can be summed and also substituted into the value of $4r^2$ found in A.40. The result is aided by using A.30 and yields:

$$4r^2 = -A^2 \frac{\nu^2}{B^2} + 4k^{-2} J_M + [J_N - J_D - k^{-2} J_H - (2J_T - J_A) \frac{md^2}{A}] \frac{2iA\nu}{B} . \qquad \text{(A.44)}$$

Several specialty terms are required to complete the

computation of $\frac{r'}{r}$. The stability factor,

$$S=\frac{A^2\nu^2}{4Bk^{-2}J_M} \qquad \text{and}$$

$$\sigma=\sqrt{1-\frac{1}{S}} \qquad \text{as well as} \qquad (A.45)$$

$$\mathbb{R}(4r^2)=\frac{-A^2\nu^2\sigma^2}{B^2}.$$

Neglecting the imaginary part, if $\frac{r'}{r}$ is computed precisely, then the denominator multiplied by its conjugate complex with a magnitude comparison leads to the same result as if neglecting the imaginary part of $4r^2$ (except for r<<1 which is a special case not discussed).

$$\frac{r'}{r}=\frac{(4r^2)'}{2(4r^2)}=\frac{(\nu^2\sigma^2)'}{2\nu^2\sigma^2}=\frac{\nu'}{\nu}+\frac{\sigma'}{\sigma}=J_D-J_A\frac{md^2}{A}+gdU^{-2}\sin\theta+\frac{\sigma'}{\sigma}. \qquad (A.46)$$

The yawing motion is then a combination of the two solutions:

$$\lambda=\sqrt{\frac{\sigma_o}{\sigma}}e^{\frac{1}{2}\int_0^p[J_D-J_N-k^{-2}J_H+J_A\frac{md^2}{A}+i\nu\frac{A}{B})\pm(-\frac{A^2}{B^2}\nu^2+4k^{-2}J_M+(J_N-J_D-k^{-2}J_H-(2J_T-J_A)\frac{md^2}{A})\frac{2i\nu A}{B})^{\frac{1}{2}}]dp} \qquad (A.47)$$

An approximation for the solution of a stable projectile is such that the ratio of the imaginary and real parts of $r\frac{r'^2}{r^2}<\frac{1}{20}$ for stable projectiles. Using the binomial theorem to express the square root,

$$r^2=a+b \rightarrow 2r=i\frac{A}{B}\nu\sigma+[J_N-J_D-k^{-2}J_H-(2J_T-J_A)\frac{md^2}{A}]/\sigma. \qquad (A.48)$$

In that case, near stability the yaw motion is given by a combination of the two solutions:

$$\lambda=\sqrt{\frac{\sigma_o}{\sigma}}e^{\frac{1}{2}\int_0^p[(J_D-J_N-k^{-2}J_H+J_A\frac{md^2}{a})\pm(J_N-J_D-k^{-2}-(2J_T-J_A)\frac{md^2}{A})/\sigma+\frac{ivA}{B}(1\pm\sigma)]dp} \qquad (A.49)$$

This was the form that was used at Aberdeen Proving Grounds for reduction of data. An alternate form for a stable projectile can be written as follows:

$$\frac{r'}{r}=\frac{(4r^2)'}{2(4r^2)}=-\frac{A^2\nu\nu'}{B^2}(-\frac{a^2\nu^2\sigma^2}{B^2})=(J_D-J_A\frac{md^2}{A})/\sigma^2, \qquad (A.50)$$

and then using equations A.43, A.44, and A.48 leads to: (A.51)

$$\lambda=e^{\frac{1}{2}\int_0^p[2J_D-J_N-k^{-2}J_H+gdU^{-2}\sin\theta-(J_D-md^2\frac{J_A}{A}+gdU^{-2}\sin\theta)/\sigma^2\pm[J_N-J_D-k^{-2}J_H-2J_T-J_A)\frac{md^2}{A}]/\sigma+[ivA(1\pm\sigma)B]]dp}$$

The criteria for stability can now be adequately discussed. A projectile is deemed to be stable if small disturbances have no permanent effect, that is, if the yawing motion does not, in the limit, depend on the initial yaw and the initial yawing motion. The yawing motion of a projectile is given as a linear combination of the two solutions of A.43 plus a particular solution, λ_p so that $\lambda=L_1\lambda_1+L_2\lambda_2+\lambda_p$.

The projectile is stable if λ_1, λ_2 decrease in magnitude so that in the limit only the particular solution λ_p remains (it becomes independent of the other terms). The particular solution need not be small though, for a large spin, the rate of precession is small, and the direction of its axis will change slowly. Since the trajectory curves downward after the apex of flight, the yaw will become larger. The question then becomes, "what are the necessary and sufficient conditions that the solutions given by A.47 approach zero as the arc length, p, increases?" One can see that the yaw will decrease if and only if the real part of the first bracket under the integral is negative and in absolute value greater than the real part of the second.

Let

$$a=(-J_D+J_N+k^{-2}J_H-J_A\frac{md^2}{A}),$$

$$b=-\frac{A^2\nu^2}{B^2}+4k^{-2}J_M, \qquad (A.52)$$

$$c=2\frac{A}{B}\nu\,[J_N-J_D-k^{-2}J_H-(2J_T-J_A)\frac{md^2}{A}] \quad \text{so that}$$

$$\lambda=\sqrt{\frac{\sigma_o}{\sigma}}\,e^{\frac{1}{2}\int_0^P[(-a+i\nu\frac{A}{B})\pm(b+ic)^{\frac{1}{2}}]dp}.$$

The condition of stability is: $a>0$

$$a>|\mathbb{R}\sqrt{b+ic}|.$$

Reformulating the stability criterion $b+ic=\sqrt{b^2+c^2}(\cos\phi+i\sin\phi)$ where $\cos\phi=\frac{b}{\sqrt{b^2+c^2}}$ and $\sin\phi=\frac{c}{\sqrt{b^2+c^2}}$. From De Moivre's theorem:

$$|\mathbb{R}\sqrt{b+ic}|=4\sqrt{b^2+c^2}\sqrt{\frac{1}{2}(1+\frac{b}{\sqrt{b^2+c^2}})}=\sqrt{\frac{1}{2}(b+\sqrt{b^2+c^2})}. \qquad (A.53)$$

So that the stability criteria become:

$$a>\sqrt{\frac{1}{2}(b+\sqrt{b^2+c^2})}$$

where

$$-a=\mathbb{R}(a_1+a_4)$$

$$b=\mathbb{R}4r^2$$

$$c=Im\,4r^2.$$

Additional steps are taken in reformulating the stability criteria in terms of aerodynamic coefficients:

$$a^2 > \frac{1}{2}(b+\sqrt{b^2+c^2}), \quad a>0$$

$$\rightarrow \; 2a^2 > b+\sqrt{b^2+c^2}, \quad a>0$$

$$\rightarrow \; 2a^2-b > \sqrt{b^2+c^2}, \quad a>0$$

$$\rightarrow \; (2a^2-b)^2 > b^2+c^2, \quad a>0$$

$$\rightarrow \; 4a^4-4a^2b > c^2, \quad a>0$$

$$\rightarrow \; -4a^2b > c^2-4a^4, \quad a>0$$

and finally, $$\rightarrow \; -b > -a^2+\frac{c^2}{4a^2}, \quad a>0. \qquad \text{(A.54)}$$

Noting that a^2 is of the order of J^2 and $\frac{c^2}{4}a^2$ is of the order $\frac{A^2}{B^2}\nu^2\frac{J^2}{J^2} = \frac{\nu^2}{100} \gg J$, $b \sim \frac{A^2}{B^2}\nu^2 \gg J$, therefore, the a's can be neglected. Let

$$b = -\frac{A^2}{B^2}\nu^2+4k^{-2}J_M, \text{ and } c = 2\frac{A}{B}\nu\cdot[J_N-J_D-k^{-2}J_H-(2J_T-J_A)\frac{md^2}{A}] \equiv 2\frac{A}{B}\nu\cdot f,$$

such that now we can rewrite inequality A.54 as

$$\frac{A^2}{B^2}\nu^2-4k^{-2}J_M > \frac{(f2\frac{A}{B}\nu)^2}{4}a^2 \equiv 1 - \frac{4B^2k^{-2}J_M}{aA^2\nu^2} > \frac{f^2}{a^2} \qquad \text{(A.55)}$$

Recalling the stability factor, S, $\frac{1}{S} \equiv \frac{4B^2k^{-2}J_M}{A^2\nu^2}$ allows the following steps:

$$a=(-J_D+J_N+k^{-2}J_H-J_A\frac{md^2}{A}) \equiv S_1$$

$$a+f=(-J_d+J_N+k^{-2}J_H-J_A\frac{md^2}{A}+(J_N-J_D-k^{-2}J_H-(2J_T-J_A)\frac{md^2}{A} \equiv S_2$$

$$a-f=(-J_d+J_N+k^{-2}J_H-J_A\frac{md^2}{A}-(J_N-J_D-k^{-2}J_H-(2J_T-J_A)\frac{md^2}{A}\equiv S_3$$

These terms S_1, S_2, S_3 are very important to the rest of the discussion of stability. The final criteria for stability is:

$$\frac{1}{s} < \frac{S_2 \cdot S_3}{S_1^2}, \qquad S_1 > 0 \tag{A.56}$$

where $$S_1 = J_N+k^{-2}J_H-J_D-J_A\frac{md^2}{A},$$

$$S_2 = 2J_N-2J_D-2J_T\frac{md^2}{A}, \tag{A.57}$$

and $$S_3 = 2k^{-2}J_H+(2J_T-2J_A)\frac{md^2}{A}.$$

Using the relationships between the S terms and f, the stability criteria can be rewritten,

$$S > \frac{S_1^2}{S_2 S_3} = \frac{S_1^2}{(S_1+f)(S_1-f)} = \frac{S_1^2}{S_1^2-f^2} = \frac{1}{1-\frac{f^2}{S_1^2}}, \quad S_1>0. \tag{A.58}$$

Then, $\lambda \propto e^{\frac{1}{2}\int_0^P [(-S_1+i2k^{-1}\sqrt{J_M}S) \pm \sqrt{b+ic}]\,dp}$

where $b=4k^{-2}J_M-\frac{A^2}{B^2}\nu^2=4k^{-2}J_M(1-\frac{A^2\nu^2}{4B^2k^{-2}J_M}) = 4k^{-2}J_M(1-S)$

$$c=2\frac{A}{B}\nu \cdot f = 2\sqrt{4k^{-2}J_M}\sqrt{S}\cdot f$$

and because S>0, it follows that S>1 from A.58. This is the "classical stability condition." This is not sufficient though. The general motion for

$$\xi = U\lambda e^{-i\int \nu\, dp},$$

with the two solutions for λ represents the superposition of the two cyclic motions, each decreasing in amplitude. This is the epicyclic motion caused by the coning and spinning simultaneously.

For S values around 1.5, the epicyclic yawing motion will have many maxima. The successive values of the yaw at maxima may increase without bound.

If the classical condition for stability is not met ($S<1$), then the final step of the inequality A.58 can not be satisfied. The yaw will grow steadily and the motion is similar to the falling motion of a top as the spin becomes too small.

It would be difficult to meet the condition $S_1<0$ since the terms J_N, $J_H \approx 10J_D$. If $J_H < 0$, then this condition could be met, but this is unlikely to happen since it would require a shift of the center of mass, which for our purposes is not practical.

Finally, the stability found in the product of the S_2, S_3 terms may be sufficient to cause instability. Recall that:

$$\frac{1}{S} < 1-\frac{F^2}{S_1^2} \text{ for } S_1>0, \quad \frac{F^2}{S_1^2} \text{ could become} > 1. \quad \frac{S_2}{S_1}=1+\frac{f}{S_1}, \quad \frac{S_3}{S_1}=1-\frac{f}{S_1}.$$

This would happen if either of the S_2, S_3 terms become negative. But, because $S_2+S_3=2S_1$, $S_2+S_3>0$, *always*. Depending on the sign of the Magnus moment coefficient, J_T, a change in magnitude could cause either S term to become negative and result in an unstable projectile.

APPENDIX B

The laser melting of a projectile surface is the alternative to multiple pulse dimples. To heat the surface to a depth of greater than 3 mm, the surface temperature profile will appear as in Figure 29 below.

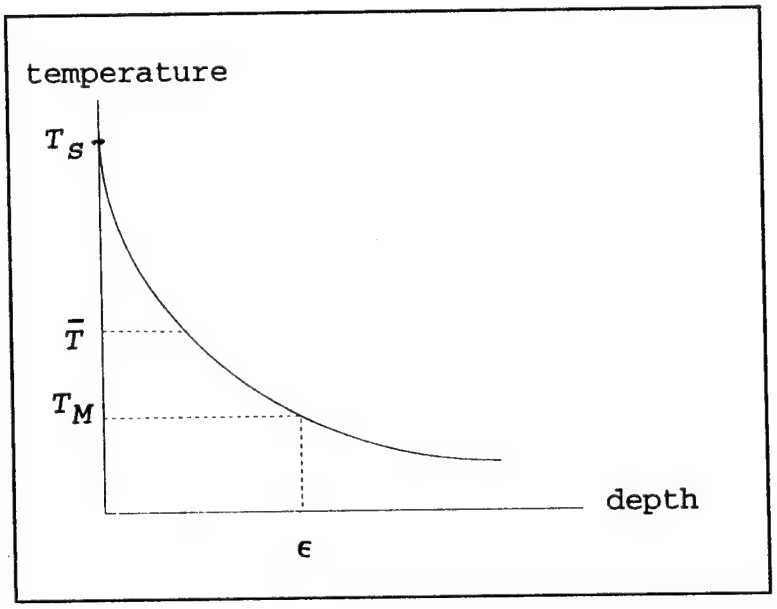

The melting temperature at a depth for steel is related to the surface temperature by:

$$T_M = \frac{T_S}{\epsilon} = 1450\ C, \quad T_S = 3900\ C. \tag{B.1}$$

The heat diffusion thickness is:

$$\epsilon = s\sqrt{\kappa t_D}, \quad \text{where } \kappa_{steel} = 0.05\frac{cm^2}{s}, \quad t_D = \left(\frac{\epsilon}{2}\right)^2 \frac{1}{\kappa} = 0.45 \text{ sec.}$$

The required heat is best deposited in a time, $t_f < t_D$. The average temperature to which the material must be raised is estimated to be:

$$\bar{T} = \frac{T_M + T_S}{2} = 2700\ C. \qquad \text{(B.2)}$$

This gives a required fluence of:

$$F_o t_f = \rho\epsilon[L_M + (\bar{T} - T_o) C_S = 4700 J/cm^2. \qquad \text{(B.3)}$$

For continuous laser illumination with a sufficiently large burn spot (radius 30 cm) on a projectile rotating with a period of 4 milliseconds, an equal distribution of the fluence is achieved.

The absorptance of steel is approximately 30% (Schriempf, 1974). This means that for a laser intensity, I_L, the fluence becomes:

$$F_o t_f = t_f \cdot 0.3 \cdot I_L = 4.7 KJ/cm^2. \qquad \text{(B.4)}$$

This gives a required laser energy of:

$$\frac{E}{\pi r^2} = 2 \times \frac{4700}{0}.3\ J/cm^2, \qquad \text{(B.5)}$$

where the factor 2 takes into account the energy required on both sides of the projectile and the factor 0.3 accounts for the reflectance. The result of solving equation B.5 for the energy is nearly 90 megajoules required. For a $t_f < 0.45$ sec, this corresponds to a laser power of 200 megawatts.

If the burn spot is reduced to an 8 centimeter radius and it is assumed the laser energy is moved over the projectile body, then substituting values into equation B.5 results in an energy requirement of only 6 megajoules and a power of 14 megawatts.

LIST OF REFERENCES

J.W. Daily, D.R.F. Harleman, Fluid Dynamics, Addison-Wesley, Inc., 1966.

R.F. Lieske, M.L. Reiter, Equations of Motion for a Modified Point Mass Trajectory, BRL Report 1314, March 1966.

E.J. McShane, J.L. Kelley, F.V. Reno, Exterior Ballistcs, The University of Denver Press, 1953.

P.E. Nielsen, Reduction of Momentum Transfer to Solid Targets by Plasma Ignition, Air Force Weapon Laboratory Laser Division Digest, LRD-72-1, p. 125, June 1972.

A.S. Platou, J. Sternberg, The Magnus Characteristics of a 30mm Aircraft Bullet, BRL Report 994, September 1956.

H.L. Power, Spinning Missile Magnus Force Measurements, Naval Postgraduate School Master's Thesis, November 1974.

J.T. Schriempf, Response of Materials to Laser Radiation, A short Course, NRL Report 7728 (1974).

F.M. White, Fluid Mechanics, McGraw-Hill, Inc., New York, 1979.

INITIAL DISTRIBUTION LIST

		No. Copies
1.	Defense Technical Information Center Cameron Station Alexandria, Virginia 22304-6145	2
2.	Library, Code 52 Naval Postgraduate School Monterey, California 93943-5002	2
3.	Professor Karlheinz Woehler, Code PH/WH Naval Postgraduate School Monterey, California 93943-5000	3
4.	Professor Michael Melich, Code PH/MM Naval Postgraduate School Monterey, California 93943-5000	2
5.	Professor Joseph Sternberg, Code PH/SN Naval Postgraduate School Monterey, California 93943-5000	1